**T E C H N I S C H E  U N I V E R S I T Ä T  B E R L I N**

Institut für Strömungsmechanik und Technische Akustik (ISTA)
Fachgebiet Dynamik instabiler Strömungen
- Hermann Föttinger Institut -
Prof. Dr.-Ing. Kilian Oberleithner

---

Diploma Thesis
(Diplomarbeit)

# PIV measurements of the far field of a turbulent swirling jet using Expancel polymer microspheres

| | |
|---|---|
| Submitted by: | Jörg Meyer |
| Field of study: | Engineering Physics |
| Matriculation number: | 183374 |
| E-Mail: | joerg.meyer@mail.com |

| | |
|---|---|
| Date: | September 30, 2018 |

| | |
|---|---|
| First supervisor: | Prof. Dr.-Ing. Kilian Oberleithner |
| Second supervisor: | Prof. Dr.-Ing. C. O. Paschereit |

## Erklärung der Selbstständigkeit

Hiermit erkläre ich, das ich die vorliegende Arbeit selbständig und eigenhändig sowie ohne unerlaubte fremde Hilfe und ausschließlich unter Verwendung der aufgeführten Quellen und Hilfsmittel angefertigt habe.

Berlin, den September 30, 2018

.....
Unterschrift (Jörg Meyer)

**Abstract**

This kind of research and investigation was made for an experimental measurement method to analysis the three-dimensional "Particle Image Velocimetry" capability with Expancel polymer microspheres as an illuminated seeding material for far field analysis in a circular turbulent swirl jet. Expancel are dry expanded polymer microspheres with a similarity in behaviour to air flow characteristics. To compare the results, all measurements are conducted at the fixed Reynolds number at Re=43k to different swirl parameters.

Zusammenfassung

Diese Arbeit befasst sich auf der experimentellen Untersuchung der dreidimensionalen "Particle Image Velocimetry" Messmethode mit Expancel polymeren Mikropartikeln als Belichtungsmaterial in einem turbulenten Fernströmungsfeld. "Expancel" sind erhitzte expandierte polymere Mikropartikelsphären mit einem äquivalentem Strömungsverhalten wie Luft. Um die Messungsergebnisse zu vergleichen wurden alle Fernfeldströmungen mit der festen Reynoldszahl Re=43k und mit unterschiedlichen Drallgrößen für den Turbulenzgrad erfasst.

# Nomenclature

| | |
|---|---|
| $Re$ | Reynolds number of the jet flow |
| $S_{local}$ | Local swirl number |
| D | Nozzle diameter |
| PIV | Particle Image Velocimetry |
| u, v, w | axial, tangential, azimutal velocity components of the fluid jet |
| x/D | measurement position ratio to the nozzle diameter |

# Contents


**1 Introduction** **4**

**2 Measurement Method and Test Facility** **5**
2.1 Swirl Jet Test Facility . . . . . 5
2.1.1 Jet Apparatus . . . . . 5
2.1.2 Particle Image Velocimetry (PIV) Setup . . . . . 7
2.1.3 Environment conditions . . . . . 10
2.2 Preliminary Work . . . . . 11
2.2.1 Basic calibrations . . . . . 11
2.2.2 Assortment of the seeding particles . . . . . 13
2.2.3 Seeding injection . . . . . 14

**3 Measurements procedure** **16**
3.1 Preliminary conditions . . . . . 16
3.2 Test Matrix . . . . . 17
3.3 VidPIV and the Software Analysis . . . . . 17
3.4 Possible measurement and analysis problems . . . . . 18

**4 Results and Discussions** **18**
4.1 Longitudinal plane - Streamwise far field . . . . . 18
4.2 Transversal plane - Crosswise far field . . . . . 24

**5 Conclusion** **39**

**6 Acknowlegments** **39**

**7 Appendix** **41**
7.1 Expancel Distributor . . . . . 41
7.2 Draeger Distributor . . . . . 41
7.3 ILA Intelligant Laser Applications Gmbh . . . . . 41
7.4 Institut für Strömungsmechanik und Technische Akustik . . . . . 41
7.5 VidPIV processing setup . . . . . 42
7.6 LDA calibration sheet . . . . . 43
7.7 Measurement Matrix sheet . . . . . 44

# 1 Introduction

At the time as I am started with this research, no one had undertaken an investigation in order to use polymer microspheres for a three-dimensional Particle Image Velocimetry measurement method (shortened: PIV). To analysis and to have a discrete characteristic behaviour for this measurement method, I chose a far field with a turbulent swirl jet, issued from a round orifice in the range of different local swirl numbers, precisely to measure and visualise plots around the vortex breakdown along a far field in streamwise and crosswise form.

All experiments are maintained with the fixed Reynolds number $Re = 43k$ to have the "simularities of motions" for a far field circular turbulent swirl jet for a better comparison between the measurements.

In the literature, described at first by Chigier and Chervinsky[1] and later by Billant[2], the similarities of motions for a turbulent swirl jet for varied swirl parameters at the vortex breakdown could be specified. The investigation of the turbulence swirl jet is arranged at the local swirl parameters $S_{local}$ = [0.6, 0.8, 1.2], which should be independently useable for any nozzle diameter, with the definition for a local swirl number

$$S_{local} = 2 * \frac{v}{u} = 2 * \frac{v_{(r/2,x=0)}}{u_{(r=0,x=0)}}$$

The motivation for choosing polymer microspheres for the seeding material was to conduct through the better illumination resolution for a far field analysis in a three-dimensional PIV measurements method compared to the established seeding oil method, which is often used in near field measurement.

# 2 Measurement Method and Test Facility

The measurements were conducted on the basis of a round orifice swirl jet testfacility in the "Fachgebiet Experimentelle Stroemungsmechanik" at the Technical University of Berlin (Appendix 7.4). All measurements of the flow field were obtained via Particle Image Velocimetry (PIV). The variation in test conditions through different local swirl numbers, were provided by adjusting two blowers aligned with a separate axial and tangential pipe, combined into a round orifice swirl generator. Each of the components of the test faciltiy will be detailed separately delineated below.

## 2.1 Swirl Jet Test Facility

The entire swirl jet test facility consists of a jet apparatus combined with a Particle Image Velocimetry system, short named as PIV. The swirling jet facility is illustrated in figure 1 and figure 3. While the jet apparatus will setup and provide the swirl jet flow for the measurements, the digital PIV system will determine the far field in its three dimensional velocity components and post-process a visualisation of the swirling flow inside the far field.

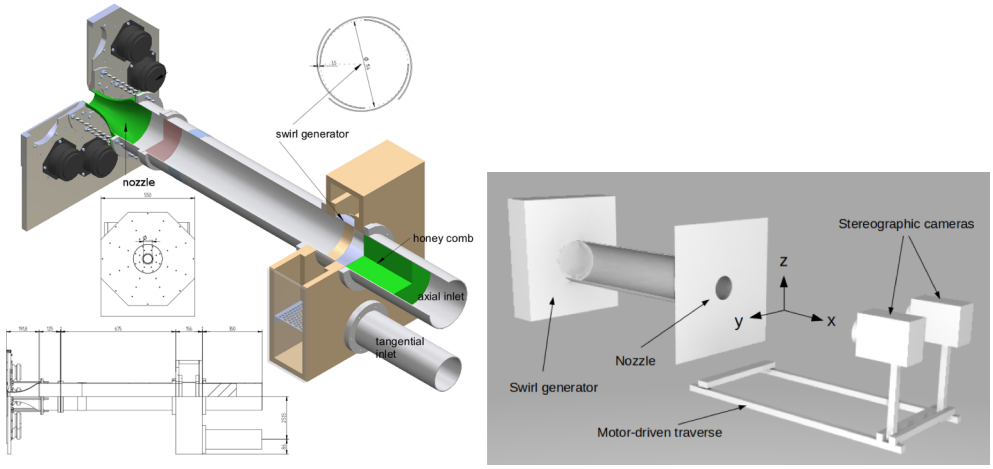


(a) inlet pipes and swirl generator (b) traverse and PIV composition

Figure 1: PIV swirl jet test facility sketch

### 2.1.1 Jet Apparatus

Through two separate inlet pipes the total volume flow could be devided in individual partial volume flows for an axial and tangential component. At the beginning of the pipes, two adjustable blowers accelerate the axial and tangential flows. The partial flow rates are measured with a pressure orifice between the blowers and the swirl generator on each pipe. That permitted an independent

control to setup the Reynolds number for the connected swirl chamber. The blowers adjustments were made via two loop controllers of the type "Siemens Micromaster 420" in combination with a HP multimeter (figure: 2b) and connected baratrons to the pressure orifice (figure: 2a). After passing a honeycomb in the axial flow, both flows enter the swirl chamber with a defined Reynolds number.

The swirl generator has two constructed areas (figure: 3a). A production chamber with an inlet for the symmetrical tangential flow, which moves through a slot system between four curved and azimuthally displaced guiding plates to the centre of the swirl generator, and a centered axial flow mixure area where is inject the new spin tangential flow onto the border of the incoming axial flow. The swirl flow then leaves the generator through an 800mm long duct pipe where an injection-hole with a seeding-generator merges the swirl flow with the seed particles, before it is converged in a nozzle and exit as a swirl jet.

(a) Blower with baraton

(b) Digital regulator with multimeter

Figure 2: Blower and regulator facility

The nozzle inlet area has a diameter of 154mm, in which the nozzle outlet area has a one inch diameter of D=25.4mm. The nozzle form is constructed as an open diminution shape. An important setup step for the test facility was the correct adjustment for the direction of the nozzle to the seeding injected pipe to prevent an offset for the PIV measurement.

(a) swirl generator side view

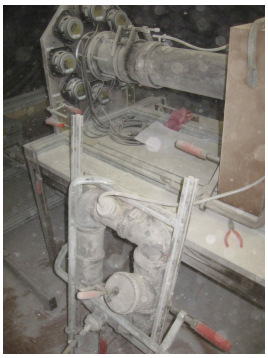

(b) seeding generator with injection position

Figure 3: swirl and seeding generator

The seeding generator was made of a combination of a circulate PVC-pipe systems (figure: 3b). On the lower side I used a pressured inlet control valve to control the seeding flux. A hatch on the side could then be used to refill the generator outside the measurement periods. The upper side of the generator was then plugged with an outlet connection with a small PVC-hose pipe to the seeding injection point near the nozzle. In order to stabilise the construction, I decided to use supplementary an aluminium-profiles framework, to hold all components together.

### 2.1.2 Particle Image Velocimetry (PIV) Setup

The far field swirl jet measurement was made via the ILA Particle Image Velocity system, shortened PIV. The system consists of a set of two CCD cameras, a high power Nd:YAG laser with a optical lens arrangement, an image processing PCI-card and a PC with the ILA software VidPIV4.6.

Additionally, a linear traverse via a serial motor-control positioned the PIV camera setup at the two different kinds of measurements for streamwise and crosswise profiles.

One notable consideration point, on how to construct the traverse, was to connect the two camera aluminium profile pylons together with the laser lens holder. The construction should not have an impact on the jet behaviour. Through construction issues of the linear motor-controlled traverse, a distance of 162cm between the pylons was selected while the laser lens holder could be mounted at the centreline 95cm in front of the pylons at the floor bottom of the linear traverse.

For the stepper motor-control on the linear traverse (protected inside the tent with foil against the seeding particles) I used an external motor driver “proMa CSD 315-S” (outside the tent), which was able to handle the ISEL-protocol on the traverse stepper motor. The motor driver was then connected serially (RS-

232) with a PC which included the freeware software Galaad3, figure:6a. In this case it was possible to have a full visual control system outside the tent for the linear motor-driven traverse, which was inside the tent with a full protection over the time against the self-agglutinating seeding material.

To calibrate the test facility for the VidPIV software, I had to construct and position a calibration map, called target, for the streamwise measurement at a position distance of 395mm in front of the nozzle end, figure: 4a. The first camera focused mapping point was 155mm in front of the nozzle on the position x/D=6.1. After that I repositioned the measurement image field area by driving the traverse to the start position x/D=3 (-75mm) for all streamwise measurements sequences. The crosswise measurements were done at the positions x/D=[1,2,...,17,16,18] and the target was calibrated directly planar on the nozzle end position.

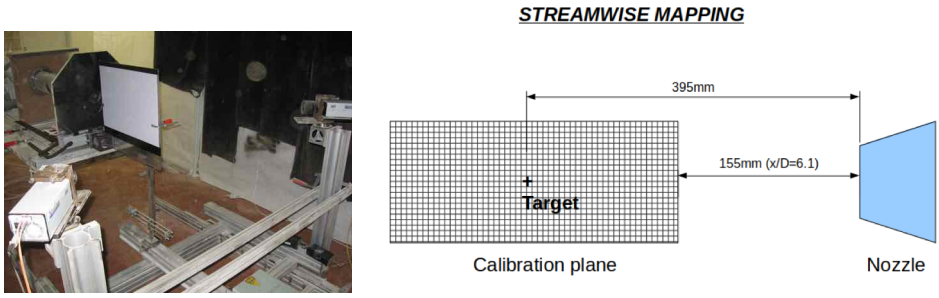


(a) laser, camera and mapping adjustment

(b) steamwise mapping position

Figure 4: streamwise measurement setup

The PIV stereoscopic camera setup was made with two ILA PCO SensiCam QE 12Bit digital double-frame CCD cameras, whereas each of them was mounted in a 50° viewing angle to a calibration plane spot on the top of the traverse. The resolution of the camera is 1280 pixels by 1024 pixels and the size of each pixel is 352.73µm (72PPI) by 352.73µm (72PPI). The minimum interframe time is 500ns and 250ns for the shutter speed between each captured frame on a single double-framed camera. 800 samples were been recorded for each measurement and each sample consists of a pair of images separated by the time interval dt=60µs. To isolate the cooling fan of the digital camera against the seeding particles, I decided to wrap a transparency foil around the cameras. A fibre optical cable, plugged inside of each camera, was used to communicate between the VidPIV PC via a special ILA image capture-processing PCI-card.

For the far field measurement, I selected two equal-specified Sigma lenses with a focus length of f=28mm for the magnification. An investigation with the VidPIV software determinated a real focus length for one lens with f=27.7mm and the other one with f=25.5mm. The non-parallel orientation of the focused image plane to both camera lenses, results in a perspective distortion of the

taken pictures. To correct this, I arranged the cameras to their lenses with the Scheimpflug angle arrangement method (figure: 5). Dependent from the traverse construction between both camera pylons with a distance 162cm, the left camera lens with the focus length f=25.5mm could be re-positioned with the scheimpflug angle 49.8° and the right one with 50° for the focus length f=27.7mm.

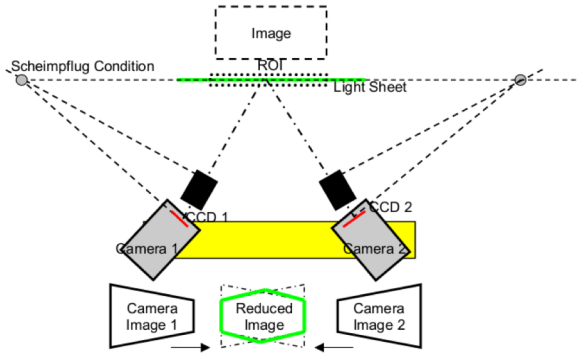


Figure 5: ILA Scheimpflug angle arrangement[3]

As well to get not optical distortions for the PIV measurements I had to clean up the lenses against the seeding particles before every new measurement sequence could be undertaken. Using a methanol filled cotton sponge with tweezers brought out the best results.

To illuminate the seeding particle flow on a wide expanded laser sheet for the far field measurement, a dual double-pulsed Nd:YAG laser emitter with a 5mm cylindrical lens and 15mJ/15Hz repetition power were mounted on the basement of the traverse-surface. For the streamwise measurement the laser sheet directed into the traverse direction on the centrelined calibration plane contrary to the transverse crosswise measurement.

The adjustment of the two laser flash lamps with a delay from 1100µs for the first one and 1160µs for the other one at the beginning measurement sequence, both with a width of 255µs and the laser Q-switch with a delay from 1250µs for the first one and 1310µs for the other one, I extend the ILA PC system (combined with the ILA VidPIV4.6 software) with an external trigger (TC412) source and connected with a external frequency generator which sourced a rising edge every 60µs.

(a) traverse software control

(b) external trigger, laser Q-switch and the VidPIV-PC

Figure 6: external electronic control elements

To not lose some luminosity of the widen laser sheet, it is to clean up the laser optics before every new measurement could be undertaken. This impact was significant, otherwise the reduced intensity decreased the capability for the VidPIV software to use the cross-correlation method.

### 2.1.3 Environment conditions

To protect the test facility, I decided to mount the entire appartus under a tent (see figure:7). In this special case for the seeding particles, the tent would also restrict the seeding dissipation locally to protect the rest of the laboratory. An additional condition for precise measurement behaviour, a tent would also reduce environmental influences. Noticeable influences could be environmental air flows (wind), air moisture and sunlight reflections, therefore it is to isolate and darken the whole tent with black cotton blankets on every wall, so it should get a good visual PIV measurement resolution. Supplementally, outside the tent, I coated over some painter's plastic foil sheets to protect the entire laboratory facilities and instruments against possible dissipate seeding particles (a point that should not be underestimated if the entire facility is not to be contaminated).

(a) inside with a LDA calibration

(b) outside with control devices

Figure 7: Tent protection without black blankets

## 2.2 Preliminary Work

### 2.2.1 Basic calibrations

Basic pre-calibrations were done separately via a coriolis-barometer to determine a calibration equation via a regression method for the pipes volume flow rates in conjunction to the baratron voltages. The results were then be scaled with an additional Laser Doppler Anemometry "LDA" measurement for the velocity components, which conducted directly at the test facility nozzle. The calibration curves together with the LDA calibration (appendix table: 7.6) defines then a ratio equation between the baratron voltages and the velocity components of the volumetric mass flow for the axial (figure: 8a) and tangential pipe flow (figure: 8b).

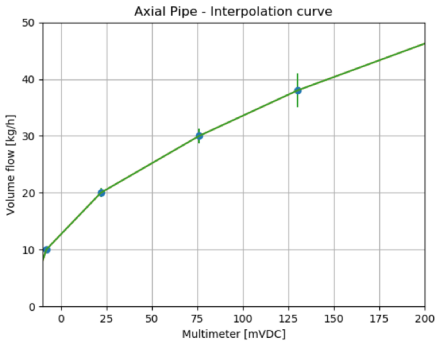


(a) axial

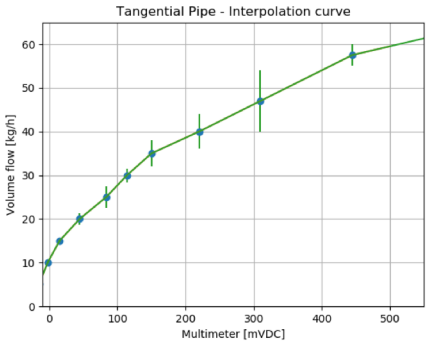


(b) tangential

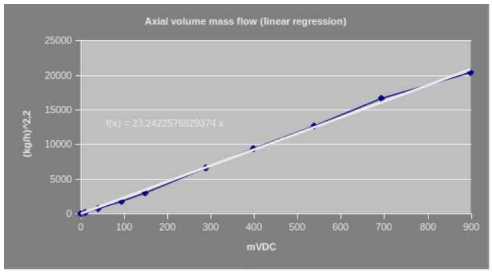


(c) axial linear

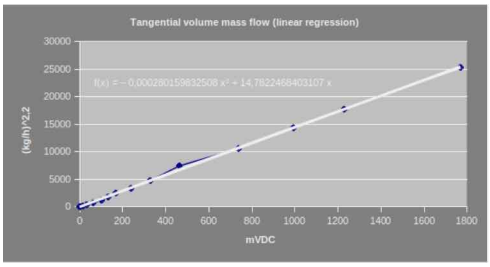


(d) tangential linear

Figure 8: calibration curves

The coriolis-barometer has a calibrated adjustment setup for the mass flow rate in kilogram per hour "$\frac{kg}{h}$", which I separately plugged into the later used tangential and axial pipe at the test facility. The different flow rates adjustments from zero to one hundred kilogram per hour were only limited through the maximum allowable voltage current rate of the also plugged baratrons.

After adjusting the coriolis-barometer, I had to set in a volumetric blend

(a) coriolis barometer with barotron, blend and multimeter (b) Laser Doppler Anemometry

Figure 9: calibration

(called orifice) of different sizes inside the pipes and connected then with the baratrons. The volumetric blends inside the pipes result in two pressure measurement points (one in front of the blend and the other one behind). Dependent on the different blend-sizes, the resulting pressure difference is induced a millivoltage direct current "$mVDC$" on the conducted baratron. A digital multimeter provides then the values from baratrons.

The results are stored into an Excel spreadsheet to compute a linear calibration curve. All volume mass flows measurements are substituted with the potency of 2.2 before a linear polynominal regression function calculates a rate function to the voltages. The resultant equation is then re-substituted with a root coefficient of 2.2 for the tangential and axial pipe and delivers a calibration equation for the barotron voltage "$mVDC$" to the tangential and axial pipe volume mass flow rate "$\frac{kg}{h}$".

On the LDA measurement, a photo detector transforms a received light particle into a voltage signal, when a particle is flying through the measuring volume. The signal is then filtered and amplified in a seperate controller to send it to a connected computer with an A/D converter. A fast Fourier transformation is computing the Doppler frequency in the signal, which is proportional to the velocity components of the particle.

To identify the dimensionless local swirl number $S_{local}$ and the Reynolds number $Re$ for the mass flow calibration equation, the velocity components of the total volume mass flow $u$ and $v$ in meter per second "$\frac{m}{s}$" are captured with a Laser Doppler Anemometry "LDA". Together with the calibration equation, all later operated measurements are at the same Reynolds number with $Re = 43k$. The local swirl number could then be determined with the given equation from Billant *et al. [2]*

$$S_{local} = 2 * \frac{v}{u} = 2 * \frac{v_{(r/2,x=0)}}{u_{(r=0,x=0)}}$$

and the Reynolds number $Re$ with the given air kinematic viscosity $\nu$ and the nozzle diameter $D$

$$Re = \frac{u*D}{\nu}$$

The local swirl number equation represents the ratio between the maximum swirl velocity to the axial core velocity at a given jet cross section in a near flow field. Therefore all LDA measurements were undertaken near at the end of the nozzle.

### 2.2.2 Assortment of the seeding particles

To select and assort the corresponding seeding material to the far field PIV measurement, I had to find out a special seeding material to the boundary condition. The usually used aerosol silica oil "DEHS" (Di-2-Ethylhexyl-Sebacat) with front scattering, which is normally used by PIV near field analysis, has only a diameter of $0.3\mu m$. But the far field anaylsis would need a more spreading seeding material as normaly chose for an near field anaylsis. Seeding the air with a larger diameter material presents a great challenge, because the air is the primarily quiescent state material (excluded wind). The ability of a particles to follow fluctuations in the air flow depends on the particle aerodynamic diameter "$d_a$" which, in turn, depends on the particle geometric diameter "$d_g$" and their density "ϱ" according to the following equation:

$$d_a = d_g * \sqrt{\rho}$$

A smaller aerodynamic diameter is associated with a higher frequency response and a greater ability to follow rapid air flow fluctuations, which depends on a particle density rate to their geometric diameter according to the equation. The selected seeding material for a far field analysis will have then a higher geometric particle diameter with a smaller density as the measured air flow.

In addition to the particle aerodynamic diameter, it is essential that the geometric diameter should not be alterable over a period of time, e.g. through dissipation.

A selection of three candidates came then into consideration. The first candidate was soap bubbles from Robert Rank with a 2-3mm diameter for the far field. Unfortunately, the biggest challenge was the expensive price for a soap sud from 500€ per 10kg. Even if the density could be similar to the air density, an additional problem lies in the double reflections from the soap bubbles for the PIV measurement. The second one was a polydisperse ethanol aerosol with front scattering, which is often used by PIV far field analysis with a diameter of 10-200µm. Unfortuantely the density of $0.8kg/m^3$ would not have the same good physical behaviour as air in the far field measuring zone with a higher diameter.

At the end I selected expanded polymeric microspheres from Akzo Nobel, called EXPANCEL. They are small spherical microsphere plastic particles with a good expanded diameter of 15-90µm and likewise physical behaviour as air

through their smaller density (filled with hydrocarbon gas). Most of the time they are used by construction companies where they are put into an isolation material. It is neither too expensive in price nor is it difficult to get a smaller quantity.

**Expancel microspheres**

Expancel microspheres are thermoplastic hollow spheres. The microspheres are white spherically formed particles with a thermoplastic shell encapsulating with hydrocarbon gas. When the microspheres are heated the thermoplastic shell softens and the hydrocarbon inside the shell increases its pressure. This results in an expansion of the spheres (typical diameter values: from 10 to 90 µm), with a decrease of the density (typical values: from 1000 to 30 g/liter) to a corresponding aerodynamic diameter similar to air. All Expancel particles are highly resilient. The expanded microspheres are easy to compress. When the pressure is reduced the microspheres regain their original volume. Due to this resiliency, Expancel microspheres can withstand without collapsing or breaking, under normal circumstances. This is very important when the microspheres are pumped from the seeding generator and mixed with the air flow at the nozzle.

To have equivalent, same physical flow behaviour as normal air, I selected the dry expanded Expancel DE microspheres particles "461 DE 20 d70" with a particle geometric diameter of 25µm for the far field seeding material.

**Disadvantage**

Beside the good Expancel behaviours for PIV measurements, there also exist some extraordinary disadvantages, which I didn't think of during the preliminary selection decisions. One dramatic impact for the PIV measurement can and is the high dependence on the humidity condition for the microspheres. It produces a lot of lumps inside the seeding flow and has an impact of the flow behaviour. At the end, the lumped microspheres agglutinated the whole equipment (pipes, barotron, blower, swirl generator, nozzle, camera lenses and the laser optic). So it is absolutely important to have dry environmental conditions for the microspheres throughout the entire test run. Before every measurement could be started, I had to dry the total laboratory facility and the Expancel microspheres. Another solution could be to have a laboratory with controllable air humidity and an air filter system for the lumped microspheres.

A special disadvantage is also the strong lung impact on the human body. Due to the microsphere density and the air like behaviour, I had to use a breathing protection system from the company Draeger, like a breathing mask with an extra fine filter grad. In this case I selected a half-mask from Draeger with a particle protection grad P2 (Appendix 7.2).

### 2.2.3 Seeding injection

Through the limitations of the disadvantages of the physical behaviours of the Expancel microsphere particles, I had to mount the injection point downstream

in the middle of the swirl flow pipe.

The first attempt to inject the seeding particles directly into the tangential blower, resulted in an agglutinated blower (figure:10a). An injection position across the axial pipe, between the baratron orifice and the honeycomb inlet to the swirl generator, also resulted in an agglutinated swirl generator. At the end I mounted the seeding particle injector downstream at the middle of the swirl flow pipe, so I could reduce the influence to the swirl jet at the nozzle (figure:10b).

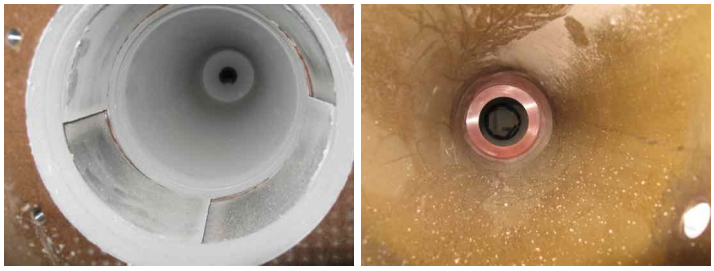

(a) forwards the swirl generator (b) afterwards the swirl generator

Figure 10: seeding injection

An additional work was conducted to develop a seeding particle generator for a constant and controllable particle flow.

The first effort was more a proof of concept, simple, fast solution with a pressurised inflated plastic bag (figure:11a). The plastic bag was controlled via an air pressured inlet pipe, which did have a separate independet manually controllable valve. The inlet was inserted into the Expancel mass to whirl up the seeding particles inside the bag. On the top of the inflated plastic bag, was then a second separate outlet pipe which was to transport the whirled particles to the injection point at the test facility. Even though this generator solution offered a constant, controllable mass flow for a short time, it wasn't able to offer a persistent constant mass flow for a running PIV measurement sequence. Through these experiences I decided to develop a simple circulated construction with plastic pipes (figure: 11b). At the head of the construction I put the outlet pipe; at the bottom, the air pressured throttle-able inlet pipe; and at the center, a refill hatch for the Expancel mixture.

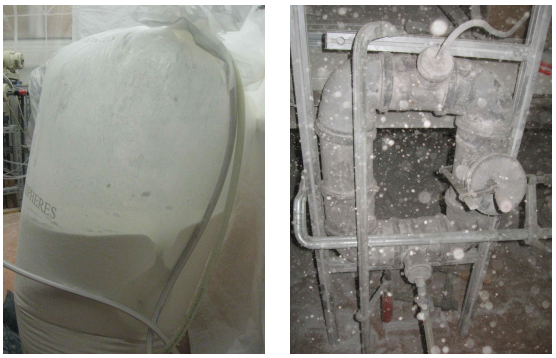

(a) first simple version (b) second enhanced version

Figure 11: seed generator versions

# 3 Measurements procedure

## 3.1 Preliminary conditions

Before any measurement could be started, I needed to dry the seeding Expancel material with a heating oven at least over twelve hours, otherwise the particles could have been wet and lumped. Every new day, after that procedure, I needed to clean up the whole test facility especially all pipes, blowers, barotrons, laser optics, swirl generator and the seeding generator from the old lumped seeding particles, before I could started with a new measurement sequence.

The baratrons needed a two hours pre-run before the pressure-voltage calibration was stabilised to the flow rate. Otherwise they intended to increase the voltage index for the same pressure value at each beginning measurement time.

Next I had to set up all the rest of the electronic components for the VidPIV software. In this case the linear traverse with the motor driver, the two camera nodes for the stereoscopic picture records, the laser optical characteristic, the external hardware trigger with 1/60µs Hz sinus frequency for the laser timing resolution and at least together with the VidPIV-PC. At last thing was to made a self pre-test with the laser and the software, to see if all is going well.

Before I refilling the seeding generator inside the tent with the new dried microspheres, I had to put on a breathing mask to protect my lungs from the microspheres for my own health. The refilling of the seeding generator with new dry particles was made before every new measurement could be started.

The last thing I have to do is to totally darken the laboratory room to reduce light distortions and to clean up all objective laser lenses and mirrors from the seeding microsphere particles.

## 3.2 Test Matrix

A series of 800 pictures with different local swirl numbers (S=0.6, 0.8, 1.2) at a Reynolds number Re=43k, were captured over two differing PIV planes (three time cross-wise and the other one time stream-wise). For continuing analysis I chose the measurement series PIV=105-108 for streamwise and the three different swirl number versions PIV=[175-190,156-171,124-139] for the crosswise planes. The first measurement sequence PIV105 were made with a streamwise plane at the swirl numbers S=*0.6* in which the other one increased the swirl number to 1.2 (PIV108). The crosswise measurements were started at PIV124 with the local swirl number S=1.2 in a series on different positions at x/D. The following measurements sequences (start at PIV156 and PIV175) with each series are decreased the swirl number until to 0.6. The full test matrix can be seen in the appendix table*:7.7*

## 3.3 VidPIV and the Software Analysis

VidPIV has the capability to setup a batch file for all computational pre- and post-processing parts to each individual measurement. The pre-processing part for the later measurement procedure can be easily coded via the main VidPIV application. This initial setup batch is then used over the measurement in which it is compute at first the calibration map into the stereoscopic perspective camera field via the deWarp function. The deWarp function transfers the resulting captures with and without the internal disparity map into an equivalent mapped view. After filtering the results once with TSAI together with and without camera coordinates and once without TSAI but with camera coordinates, it is possible to calculate the average particle values of each node by a sequence of aligned calculations over the captured deWarped pictures. The aligned calculations repeated a three time loop for cross-correlations, local velocity filters and interpolations.

To normalise the units of the velocity components into m/s, it is post-processed the measurements results with an extra VidPIV batch. The results were then stored as a numbered PIV sequence (e.g. PIV105) for further plots and analysis post-processings. The full software setup for the measurement procedure can be seen in the appendix figure 7.5.

All further post-processings for the visual plots were then performed with the numerical analysis software “Spyder”, a python Matlab alternative. At first, a script was done to compute the mean values for all PIV results. Afterward all visualisation plots could be done with different plotting scripts. For a better visualisation, the crosswise results were plotted in an u,v,w-profile at different positions x/D=[1,2,...,15] and streamwise at the positions x/D=[6,7,...,18].

### 3.4 Possible measurement and analysis problems

Through a different hardware production (two different manufactures) a false like two different lenses focal length for the camera objectives, (e.g. official specifications are f=27mm, but in reality one of the two lenses would have possibly a f=25mm focal length) would result in an inaccurate measurement and result analysis. An inaccurate planar setup about some 0,5mm difference for the traverse setup to the nozzle, could also result in a precession mistake for the later post-computational part of the correlation procedure. the same mistake can be happen if a not fully accurate printed calibration map (under $\mp$0.1mm tolerance) will be used or the mapping plane was not absolutely planar. After a while, during the measurement term, some microparticles could be stuck or reflected in the front of a camera lens.

## 4 Results and Discussions

The velocity fields from the VidPIV measurements are averaged to obtain the mean flow. The streamwise and crosswise velocity components and the RMS velocity fluctuations of the axial and tangential components are given for the Reynolds number equal at $Re = 43k$.

### 4.1 Longitudinal plane - Streamwise far field

First I will visualise the flow on the longitudinal plane via a contour plot as a stream-wise far field for each individual measurement sequence. The streamwise contour plots are for the axial, tangential and azimuthal (u, v, w) velocity components for the given swirl parameters $S_{local}$=0.6, 0.8, 1.2 . The jet spreed is gradually increased whereas the length of the potential core is reduced.

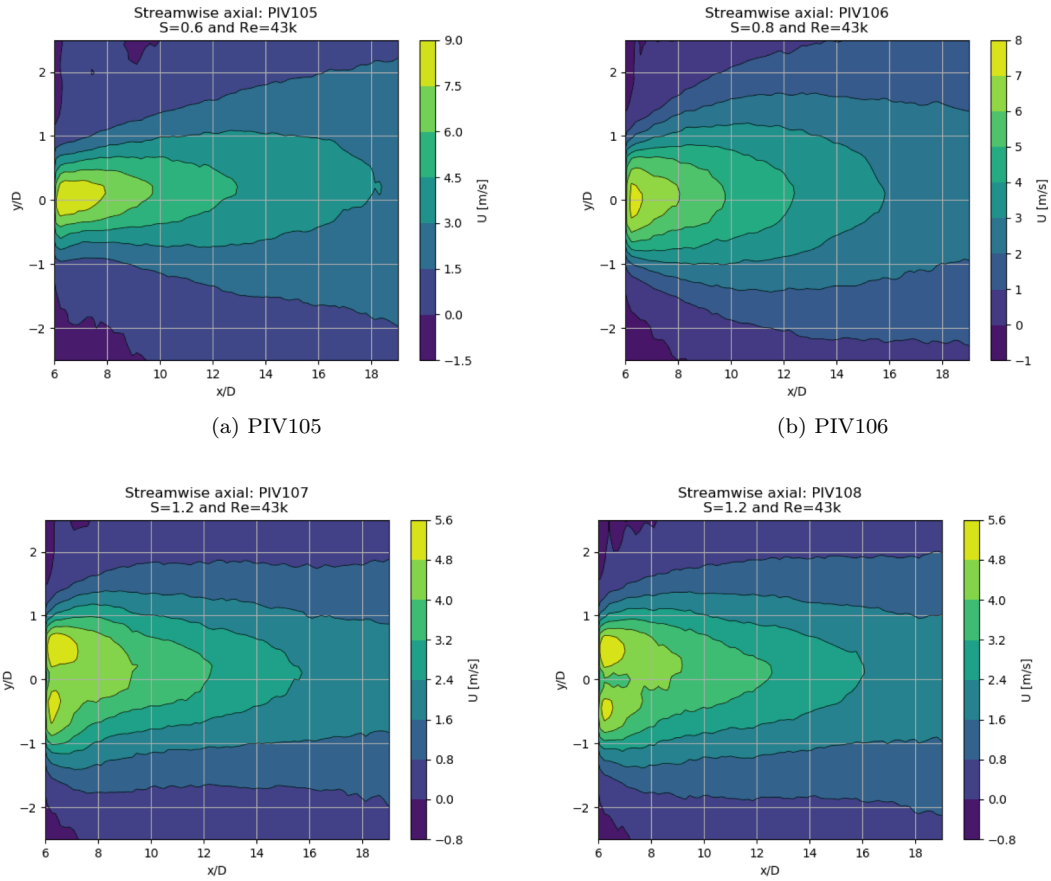


(a) PIV105

(b) PIV106

(c) PIV107

(d) PIV108

Figure 12: axial velocity component u in [m/s] with $S_{local} = [0.6, 0.8, 1.2]$

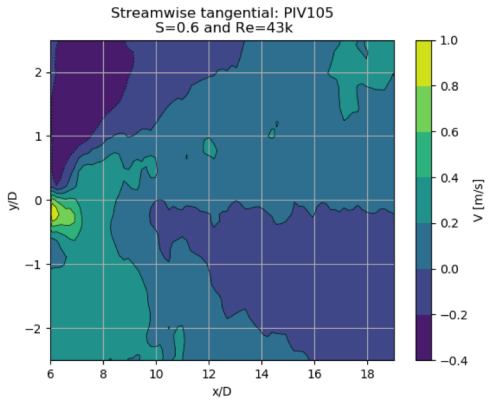


(a) PIV105

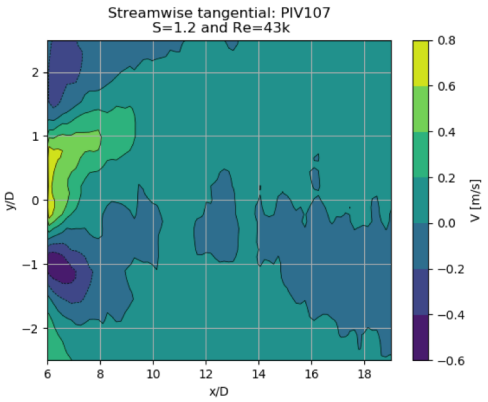


(b) PIV106

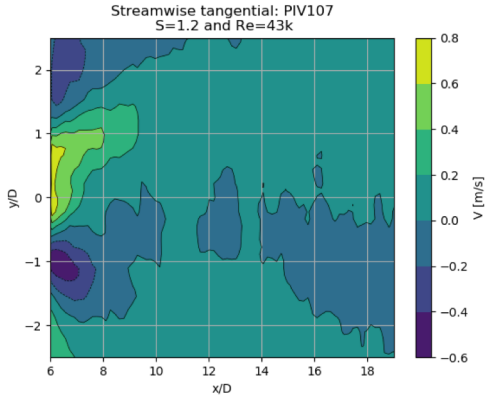


(c) PIV107

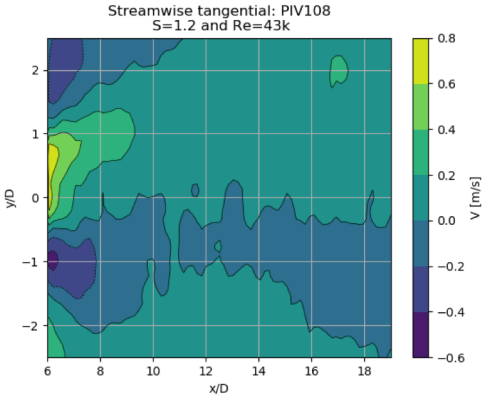


(d) PIV108

Figure 13: tangential velocity component v in [m/s] with $S_{local} = [0.6, 0.8, 1.2]$

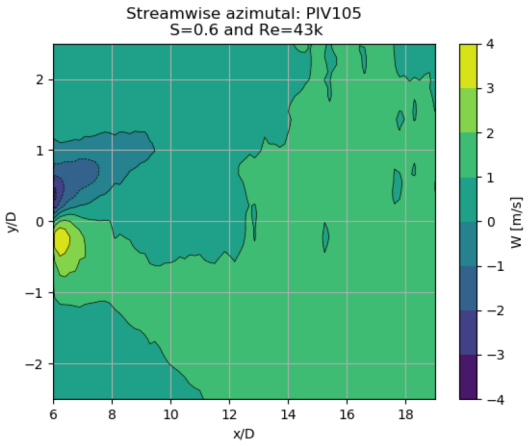


(a) PIV105

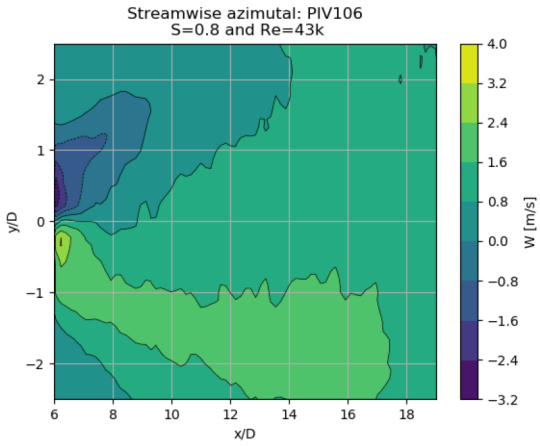


(b) PIV106

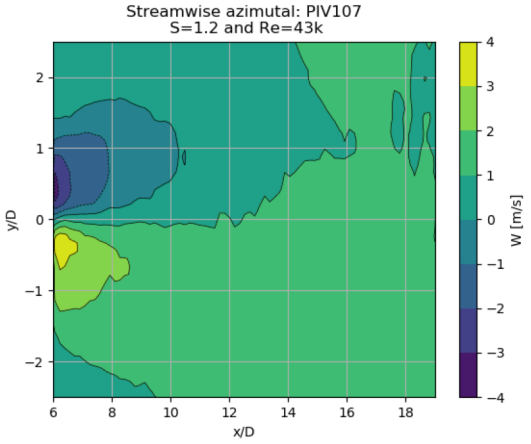


(c) PIV107

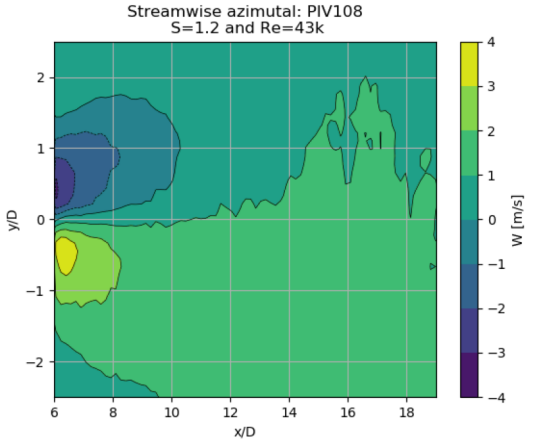


(d) PIV108

Figure 14: azimutal velocitiy component w in [m/s] with $S_{local} = [0.6, 0.8, 1.2]$

Better analysis results are observed with plots of the streamwise mean velocity components $U_{mean}$, $V_{mean}$ and $W_{mean}$ with the corresponding RMS fluctuation at a different local swirl numbers S=0.6, S=0.8 and S=1.2:

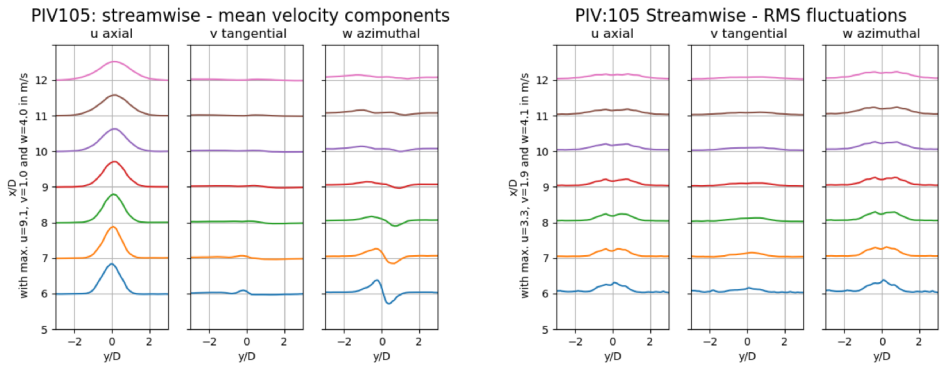


(a) mean velocity components (b) RMS fluctuation

Figure 15: PIV105 (S=0.6). Mean velocity and RMS fluctuation

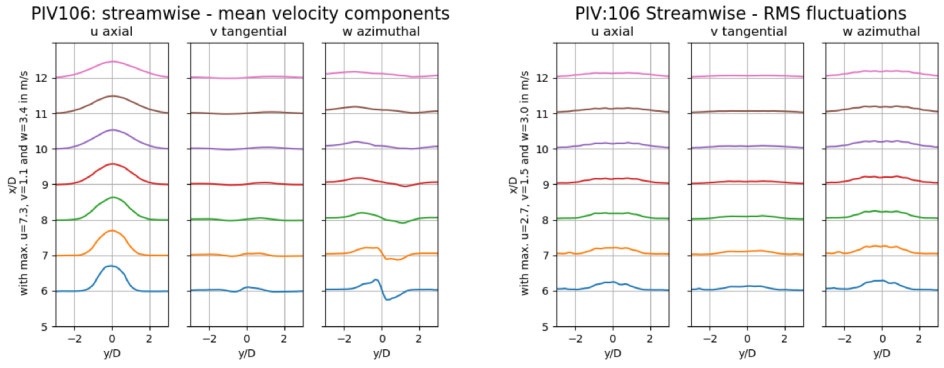


(a) mean velocities (b) RMS fluctuation

Figure 16: PIV106 (S=0.8). Mean velocity and RMS fluctuation

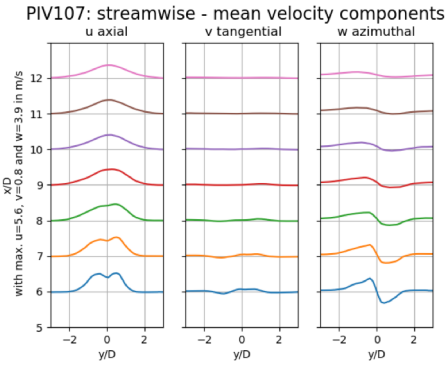


(a) mean velocities

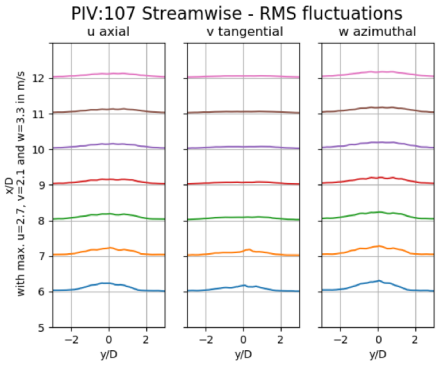


(b) RMS fluctuation

Figure 17: PIV107 (S=1.2). Mean velocity and RMS fluctuation

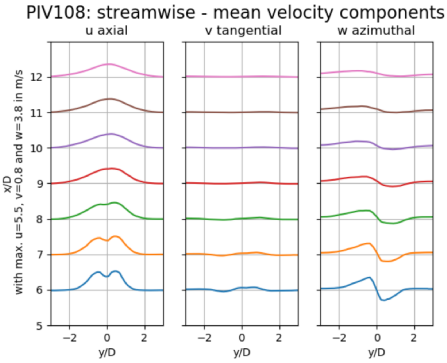


(a) mean velocities

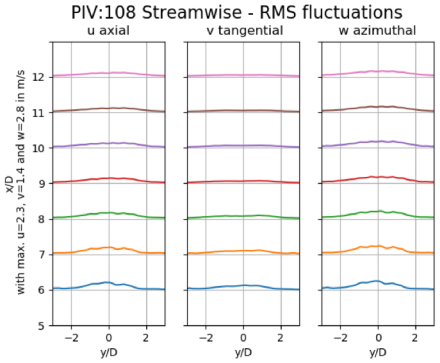


(b) RMS fluctuation

Figure 18: PIV108 (S=1.2). Mean velocity and RMS fluctuation

## 4.2 Transversal plane - Crosswise far field

The same visualisations are made on the transversal plane - crosswise far field. The crosswise vertices visualisation is setted on the cross-section along the transversal plane with a Reynolds number equal to 43k and with the local swirl numbers arranged for S=0.6, 0.8 and 1.2 (PIV:175-190,156-171,124-139)

The first plots are presenting the measured vectorfields for the axial-tangential velocity components in m/s for different arranged swirl parameters.

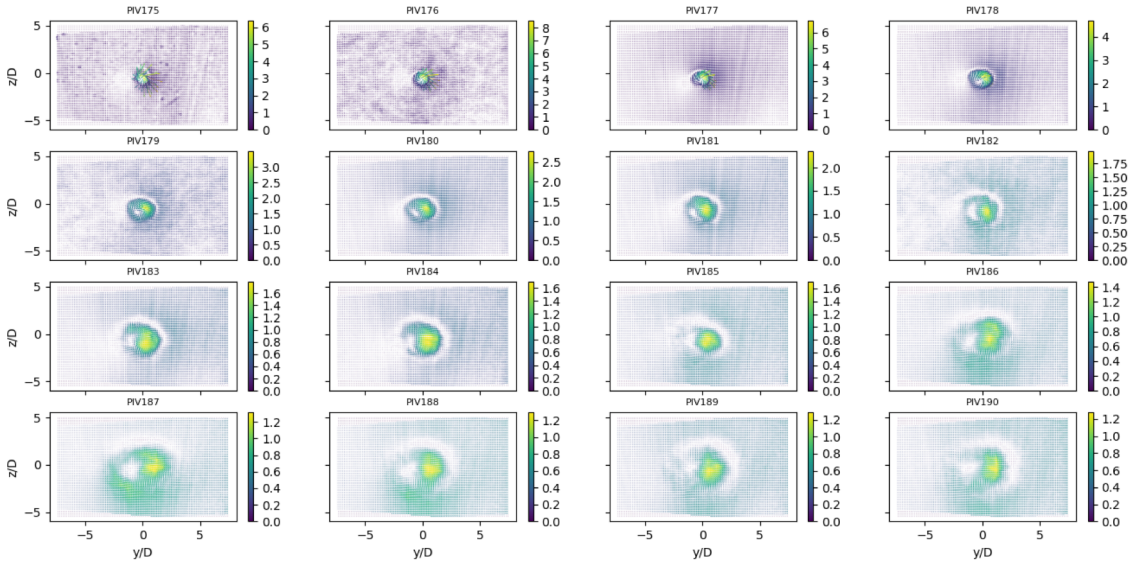


Figure 19: axial-tangential velocity vector field in [m/s] for S=0.6

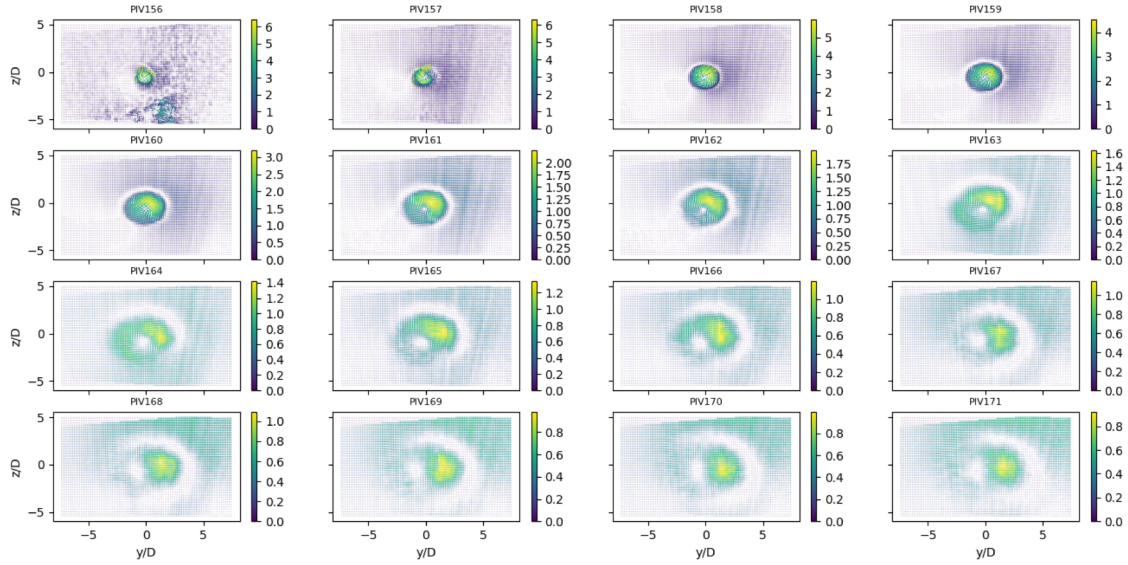


Figure 20: axial-tangential velocity vector field in [m/s] for S=0.8

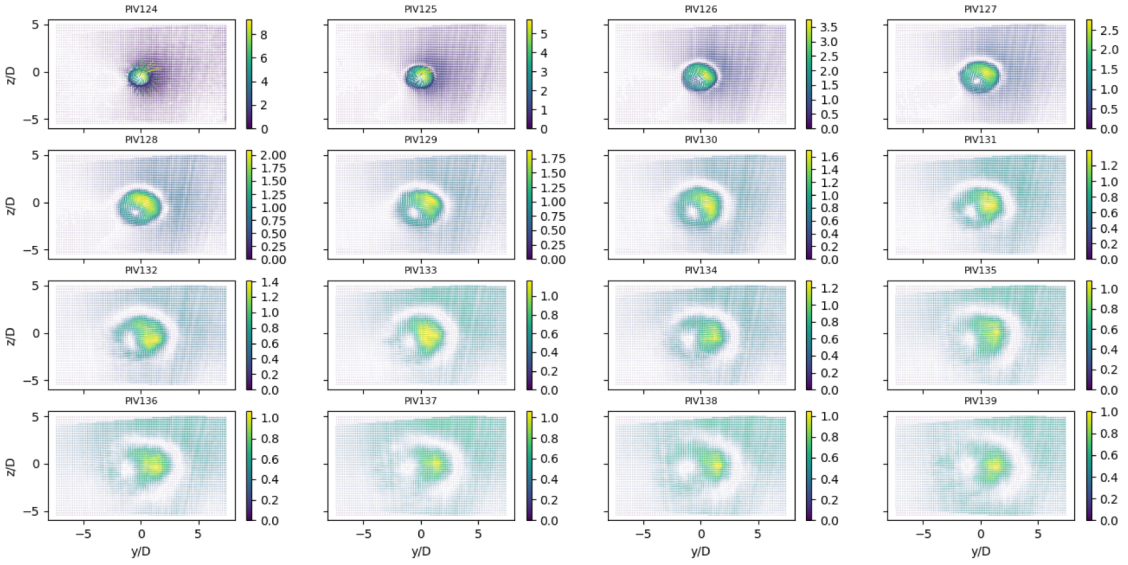


Figure 21: axial-tangential velocity vector field in [m/s] for S=1.2

More detailed informations are investigated by the crosswise profile plot $u_{mean}$, $v_{mean}$ and $w_{mean}$ mean velocity components and there flow fields at each individual cross-section sequence alone.

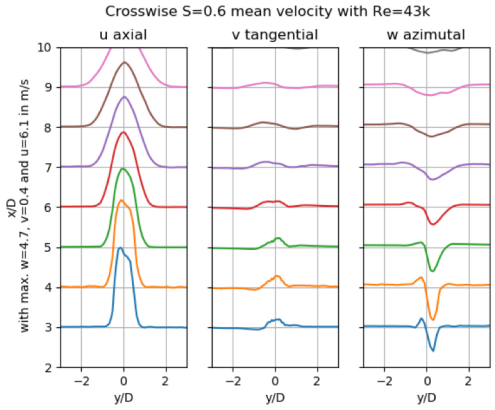


(a) S=0.6

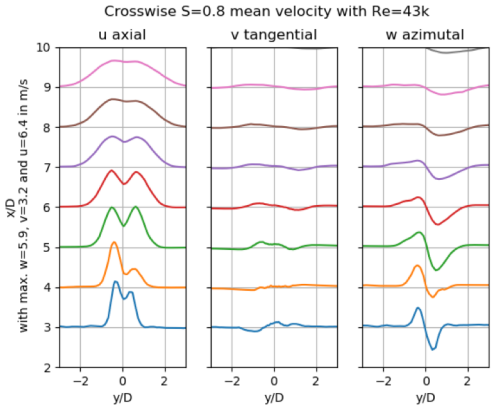


(b) S=0.8

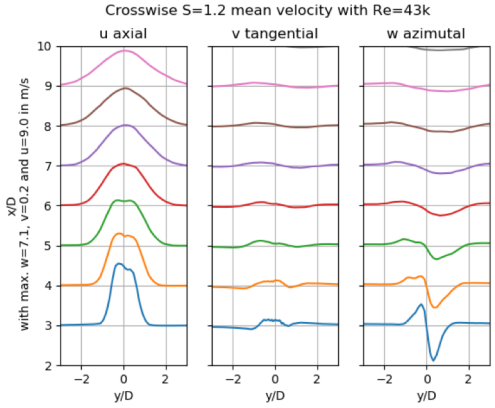


(c) S=1.2

Figure 22: crosswise mean velocity profiles, Re=43k

The Contour plots PIV175-189 are shown for every second sequence of the cross-sections with the correlated velocity components in axial, tangential and azimuthal in [m/s] for given local swirl number S=0.6

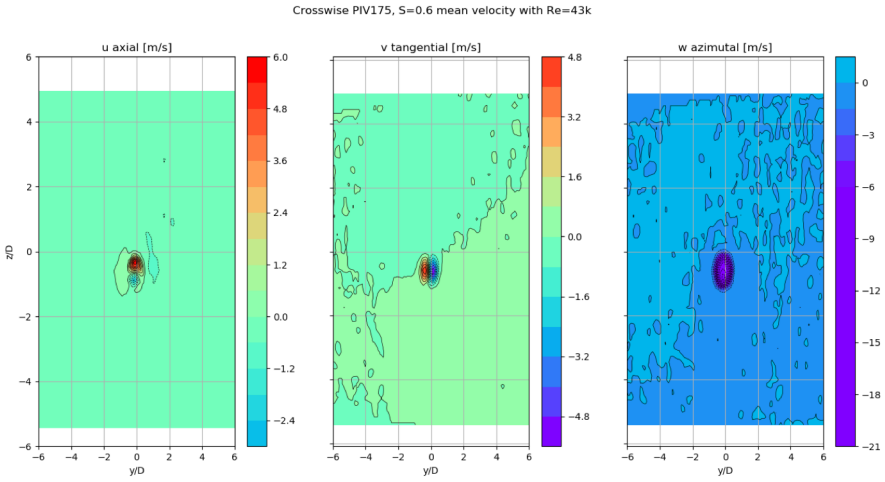


Figure 23: PIV175 at x/D=1

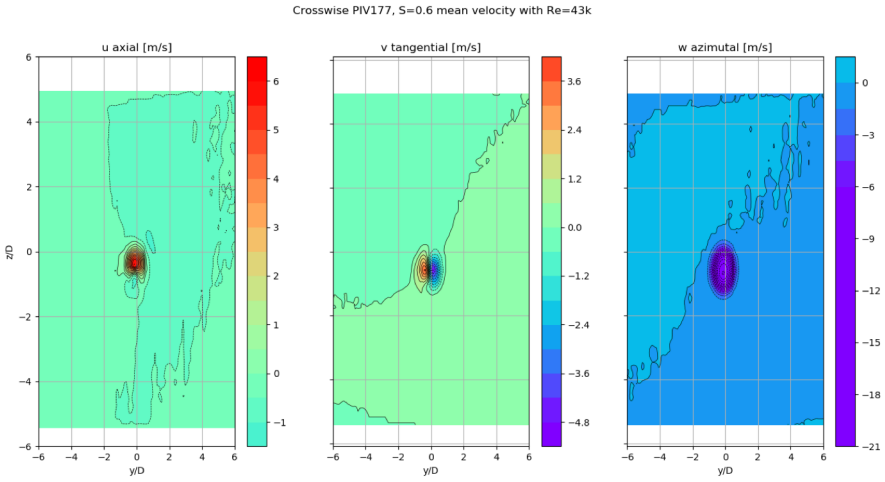


Figure 24: PIV177 at x/D=3

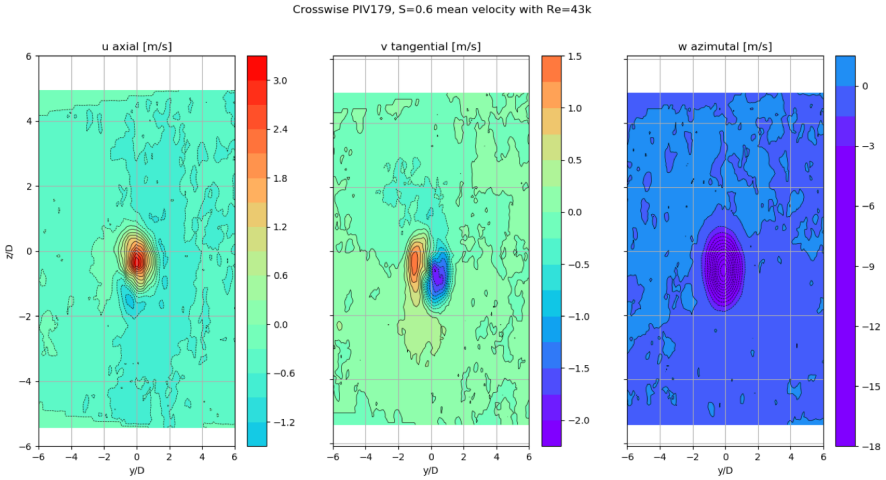


Figure 25: PIV179 at x/D=5

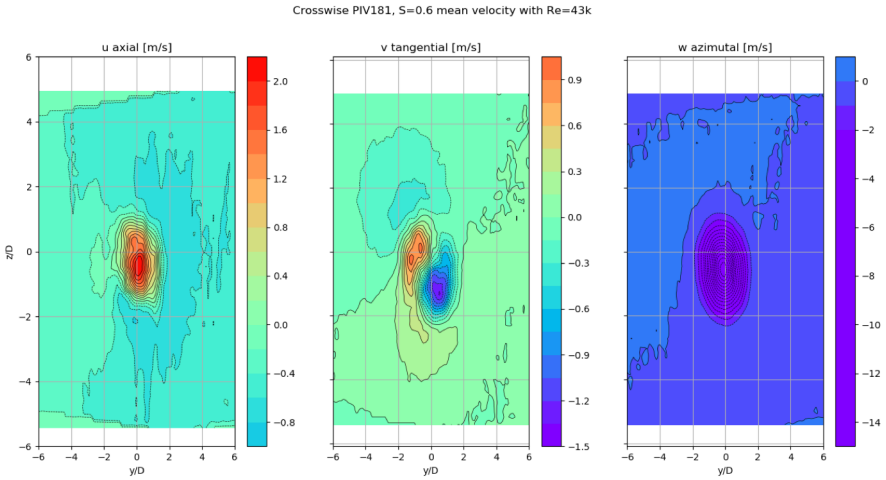


Figure 26: PIV181 at x/D=7

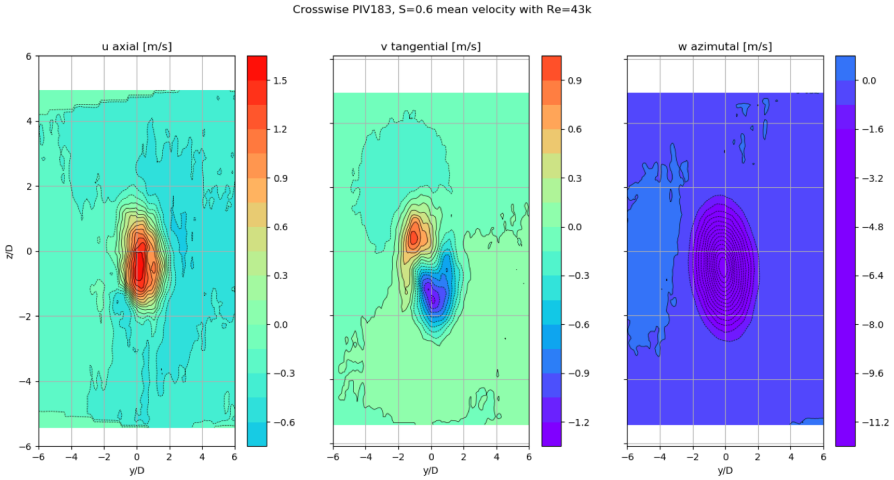


Figure 27: PIV183 at x/D=9

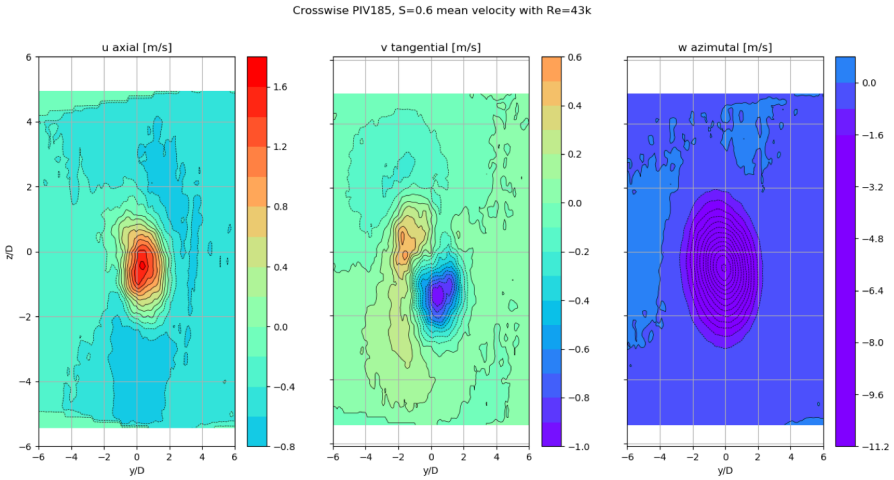


Figure 28: PIV185 at x/D=11

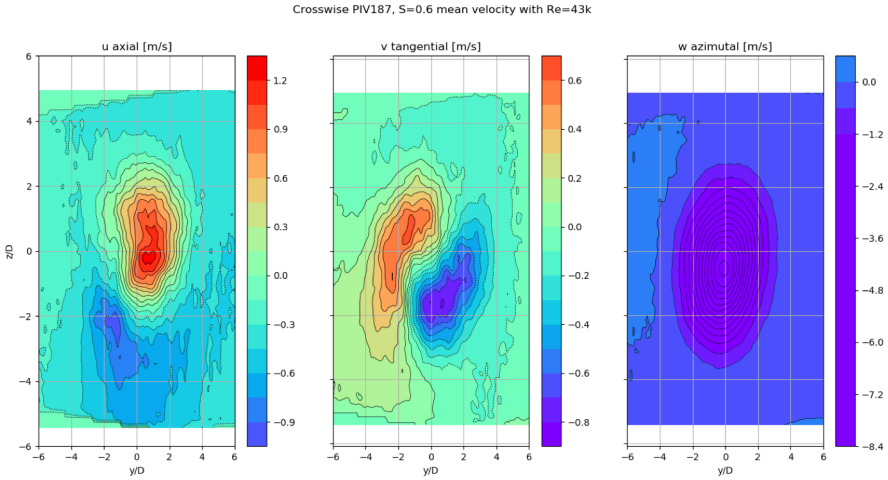


Figure 29: PIV187 at x/D=13

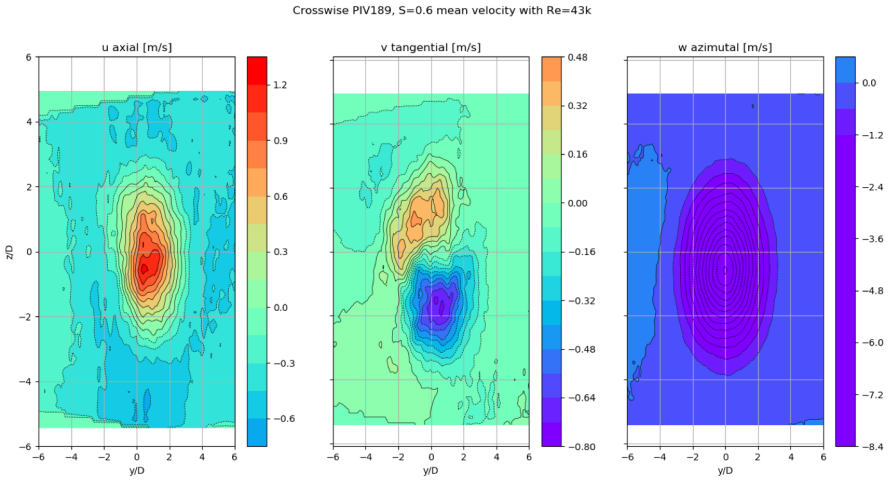


Figure 30: PIV189 at x/D=15

With the given local swirl number S=0.8, plots are made only with every second position for PIV156-170

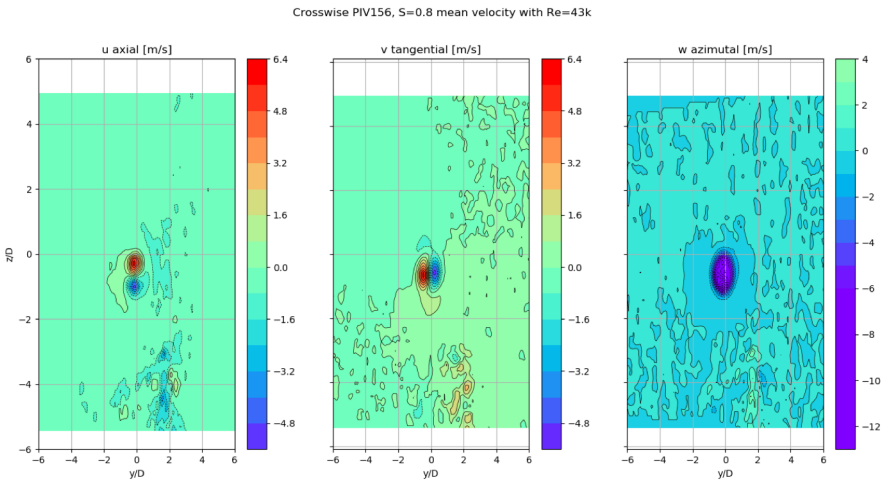


Figure 31: PIV156 at x/D=1

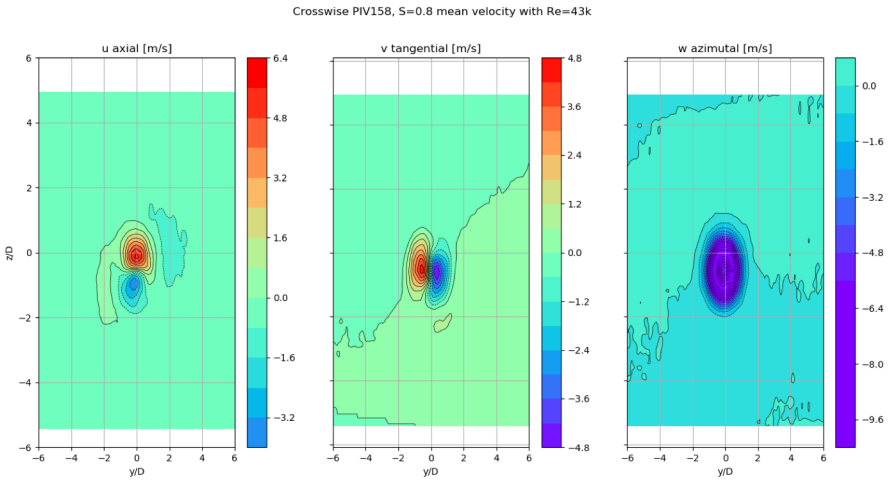


Figure 32: PIV158 at x/D=3

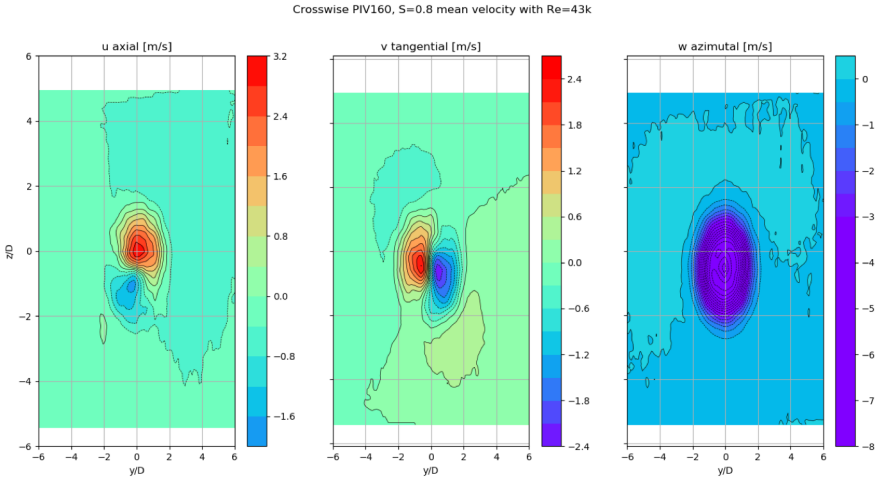


Figure 33: PIV160 at x/D=5

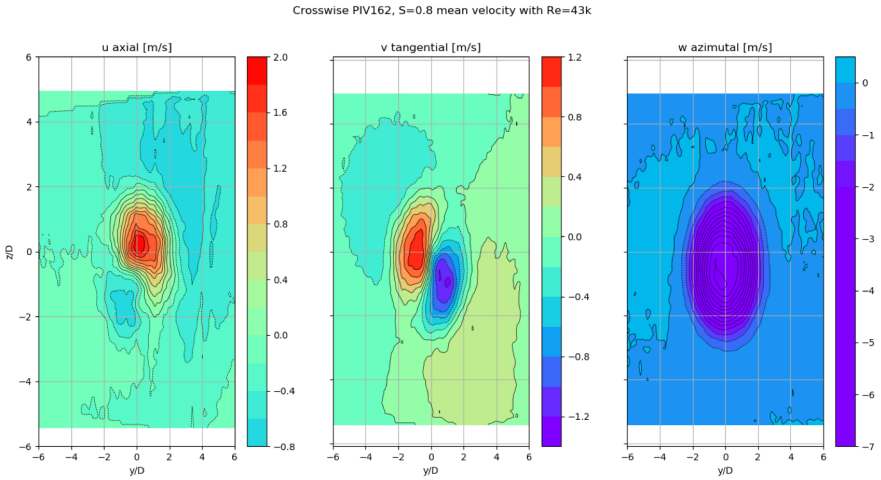


Figure 34: PIV162 at x/D=7

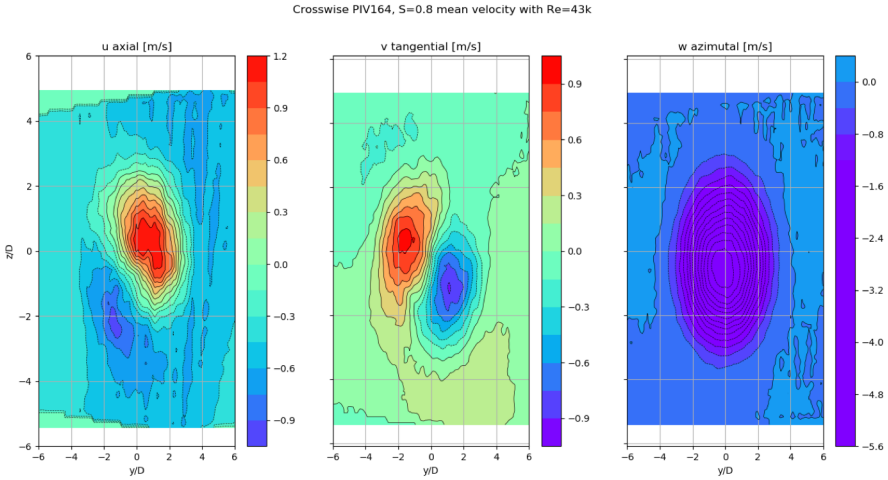


Figure 35: PIV164 at x/D=9

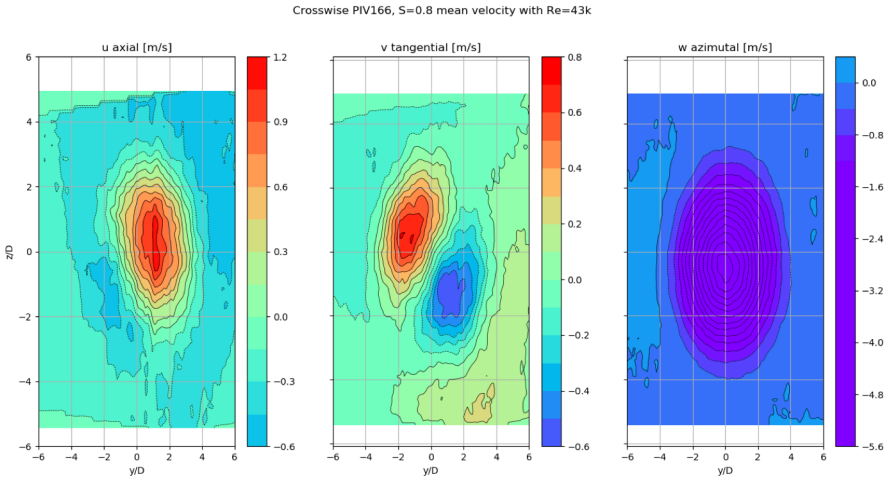


Figure 36: PIV166 at x/D=11

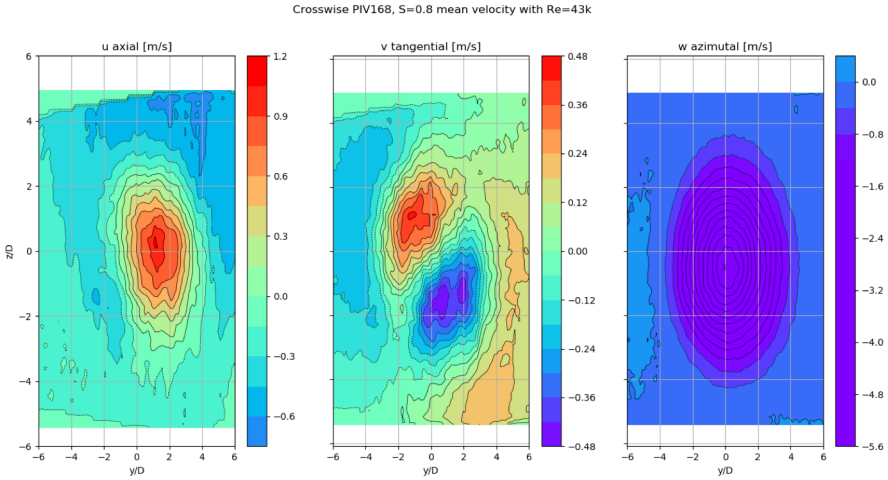


Figure 37: PIV168 at x/D=13

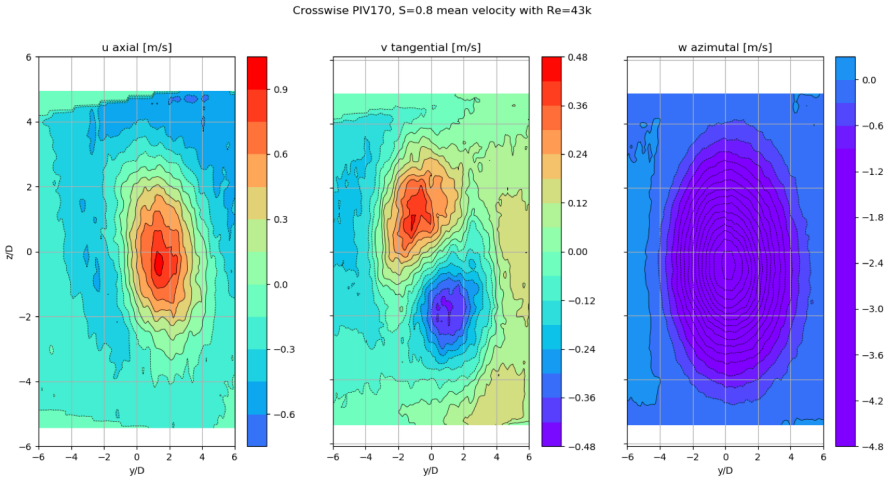


Figure 38: PIV170 at x/D=15

And for the given local swirl number S=1.2, plots are made only with every second position for PIV124-139.

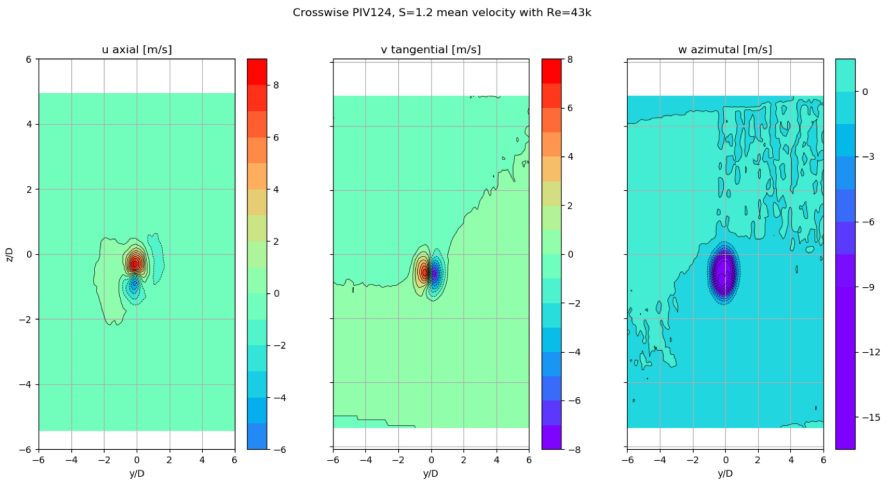


Figure 39: PIV124 at x/D=1

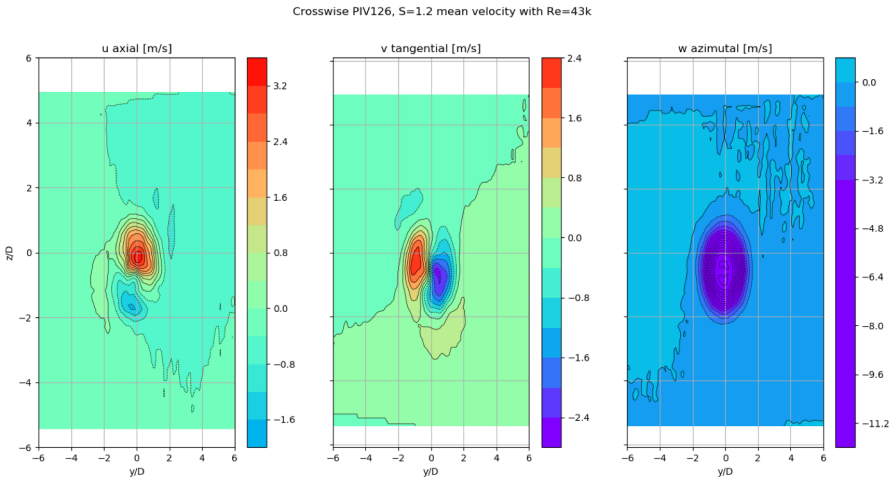


Figure 40: PIV126 at x/D=3

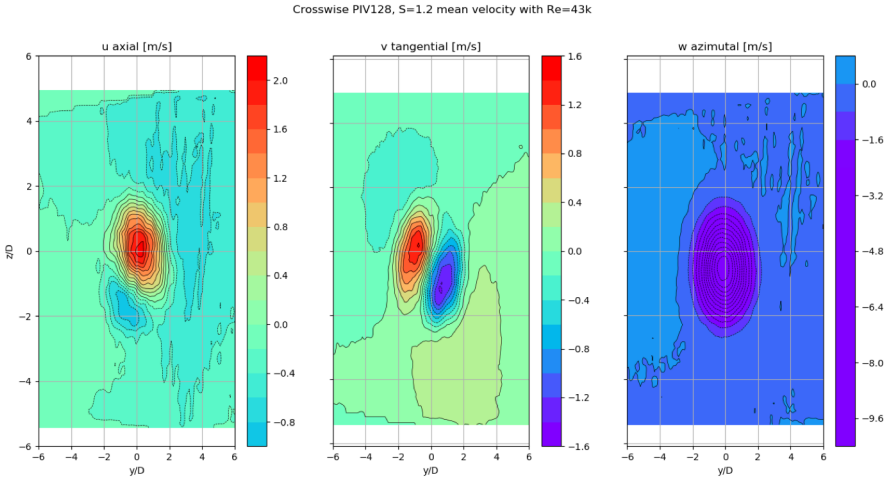


Figure 41: PIV128 at x/D=5

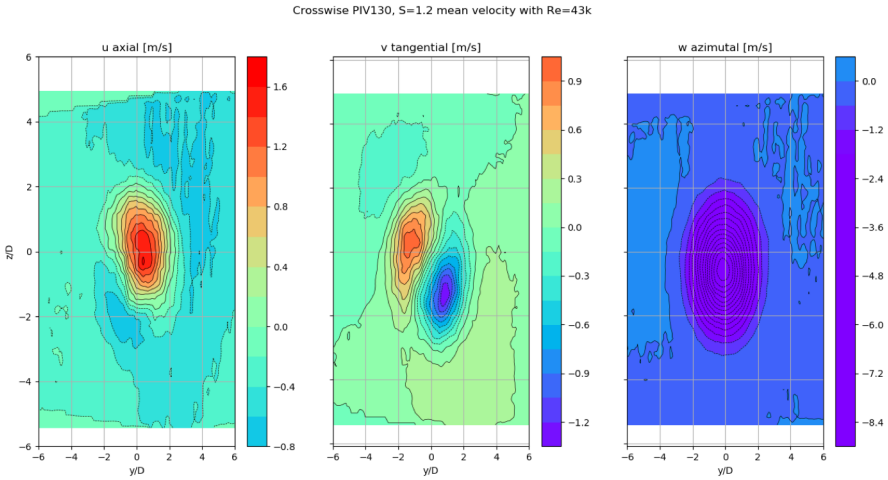


Figure 42: PIV130 at x/D=7

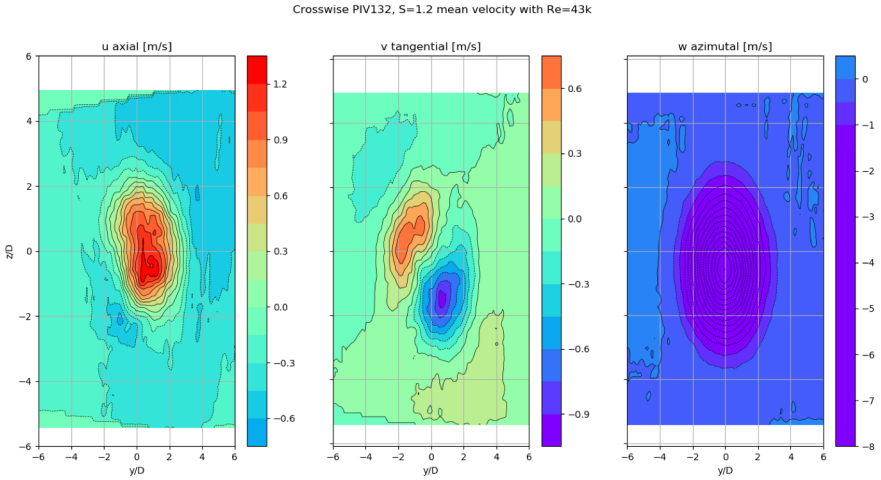


Figure 43: PIV132 at x/D=9

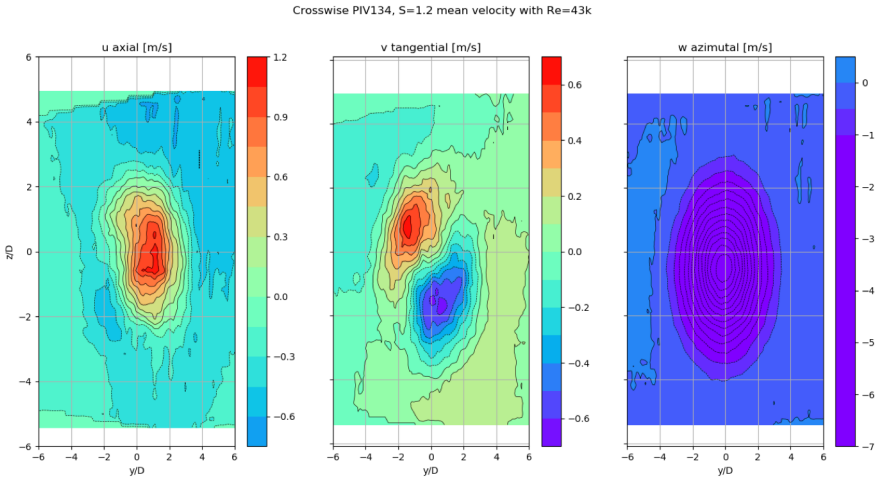


Figure 44: PIV134 at x/D=11

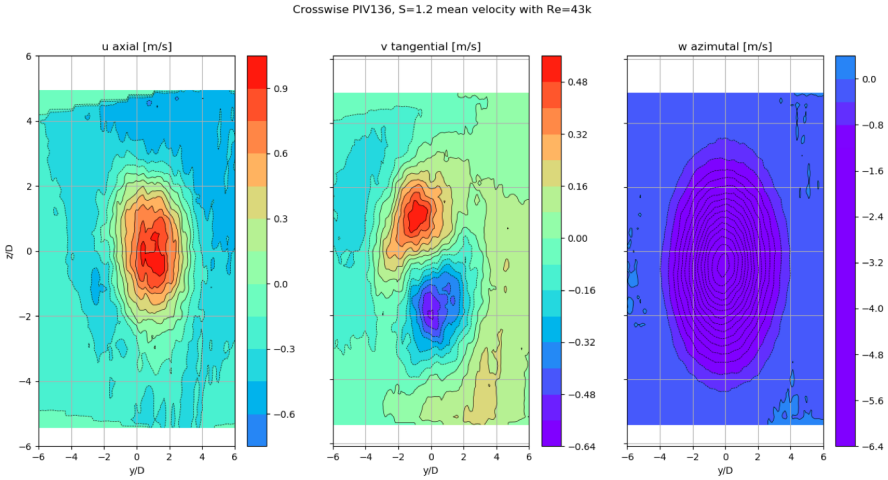


Figure 45: PIV136 at x/D=13

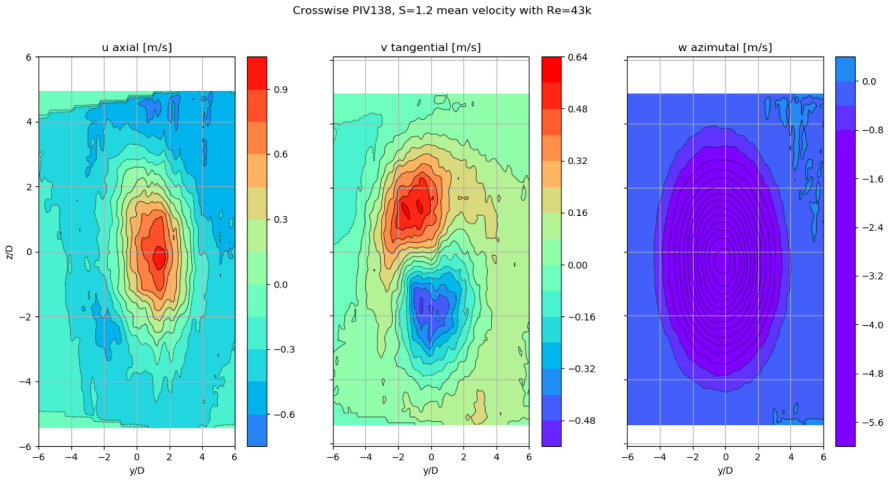


Figure 46: PIV138 at x/D=15

# 5 Conclusion

As we could see, the usage of Expancel polymer microsphere has some advantages and disadvantages. The main task to have a high illuminated contrast resolution of a far field in a three-dimensional PIV system could been full fitted. Unfortunately, the handling behaviour during the measurements was much more complicated as to expected at the beginning. But all I can confirm for the conclusion, that the main task was fully equipped, but for future measurements, some additonal preparations for the test facilities and for the environment conditions inside the laboratory have to be taken e.g. extra air filter and constant dry environment climatisation!

# 6 Acknowlegments

The research and experiments have been supported by the Institut für Strömungsmechanik und Technische Akustik at the Technical University of Berlin, Germany. Special acknowlegment to Prof. Dr. -Ing. Kilian Oberleithner for his assistance and time.

# References

[1] Chigier, N.A. and Chervinsky, A., 1965. Experimental and theoretical study of turbulent swirling jets issuing from a round orifice. Isr. J. Technol.

[2] Billant P., Chomaz J.M. and Huerre P., 1997. Experimental study of vortex breakdown in swirling jets.

[3] ILA Intelligent Laser Application GmbH. Manual script “Stereoscopic Image Correction”.

# List of Figures


1 PIV swirl jet test facility sketch . . . . . 5
2 Blower and regulator facility . . . . . 6
3 swirl and seeding generator . . . . . 7
4 streamwise measurement setup . . . . . 8
5 ILA Scheimpflug angle arrangement[3] . . . . . 9
6 external electronic control elements . . . . . 10
7 Tent protection without black blankets . . . . . 10
8 calibration curves . . . . . 11
9 calibration . . . . . 12
10 seeding injection . . . . . 15
11 seed generator versions . . . . . 16
12 axial velocity component u in [m/s] with $S_{local} = [0.6, 0.8, 1.2]$ . . 19
13 tangential velocity component v in [m/s] with $S_{local} = [0.6, 0.8, 1.2]$ 20
14 azimutal veloctiy component w in [m/s] with $S_{local} = [0.6, 0.8, 1.2]$ 21
15 PIV105 (S=0.6). Mean velocity and RMS fluctuation . . . . . 22
16 PIV106 (S=0.8). Mean velocity and RMS fluctuation . . . . . 22
17 PIV107 (S=1.2). Mean velocity and RMS fluctuation . . . . . 23
18 PIV108 (S=1.2). Mean velocity and RMS fluctuation . . . . . 23
19 axial-tangential velocity vector field in [m/s] for S=0.6 . . . . . 24
20 axial-tangential velocity vector field in [m/s] for S=0.8 . . . . . 25
21 axial-tangential velocity vector field in [m/s] for S=1.2 . . . . . 25
22 crosswise mean velocity profiles, Re=43k . . . . . 26
23 PIV175 at x/D=1 . . . . . 27
24 PIV177 at x/D=3 . . . . . 27
25 PIV179 at x/D=5 . . . . . 28
26 PIV181 at x/D=7 . . . . . 28
27 PIV183 at x/D=9 . . . . . 29
28 PIV185 at x/D=11 . . . . . 29
29 PIV187 at x/D=13 . . . . . 30
30 PIV189 at x/D=15 . . . . . 30
31 PIV156 at x/D=1 . . . . . 31
32 PIV158 at x/D=3 . . . . . 31
33 PIV160 at x/D=5 . . . . . 32
34 PIV162 at x/D=7 . . . . . 32
35 PIV164 at x/D=9 . . . . . 33
36 PIV166 at x/D=11 . . . . . 33
37 PIV168 at x/D=13 . . . . . 34
38 PIV170 at x/D=15 . . . . . 34
39 PIV124 at x/D=1 . . . . . 35
40 PIV126 at x/D=3 . . . . . 35
41 PIV128 at x/D=5 . . . . . 36
42 PIV130 at x/D=7 . . . . . 36
43 PIV132 at x/D=9 . . . . . 37
44 PIV134 at x/D=11 . . . . . 37

45 PIV136 at x/D=13 . . . . . 38
46 PIV138 at x/D=15 . . . . . 38
47 VidPIV screen . . . . . 42

# 7 Appendix

## 7.1 Expancel Distributor

CHG Chemiehandelsgesellschaft Duroplast GmbH., Kurfürstendamm 40-41, 10719 Berlin, Germany

EXPANCEL 461 DE 20 d70 - dry expanded microspheres
Density 70 kg/m$^3$
Particle Size 15.0 - 25.0 µm

## 7.2 Draeger Distributor

Loewe C.a. GmbH & Co. KG, Alt-Moabit 130, 10557 Berlin

## 7.3 ILA Intelligant Laser Applications Gmbh

TZ Jülich, Karl-Heinz Beckurts Str.13, 52428 Jülich, Germany

## 7.4 Institut für Strömungsmechanik und Technische Akustik

Fachgebiet Experimentelle Strömungsmechanik Institut für Strömungsmechanik und Technische Akustik (ehemals Hermann-Föttinger Institut), Leitung: Prof. Dr. Christian Oliver Paschereit, Müller-Breslau-Str. 8, 10623 Berlin, Germany

## 7.5 VidPIV processing setup

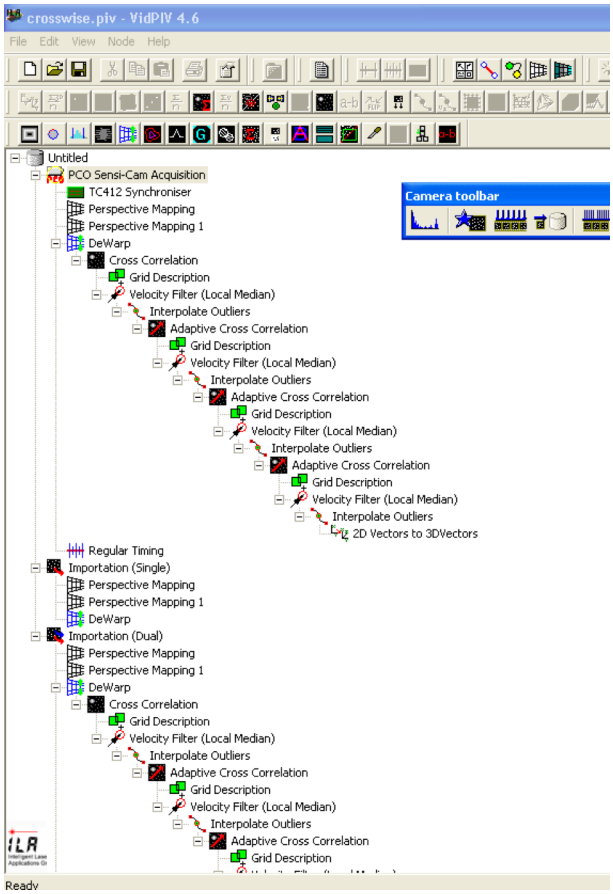


Figure 47: VidPIV screen

## 7.6 LDA calibration sheet

| Total Vol.flow | Mean Velocity | Re | u | v |
|---|---|---|---|---|
| kg/h | m/s | | m/s | m/s |
| | | | | |
| 60,80 | 27,68 | 46873,31 | 26,4 | 1,5 |
| 59,84 | 27,25 | 46135,58 | 26 | 3,5 |
| 58,70 | 26,73 | 45260,64 | 26,4 | 5,3 |
| 58,71 | 26,73 | 45262,50 | 27 | 6,9 |
| 57,20 | 26,04 | 44098,02 | 27,7 | 8,3 |
| 54,96 | 25,02 | 42370,76 | 28 | 9,3 |
| 53,65 | 24,43 | 41367,43 | 29,5 | 11,6 |
| 54,02 | 24,60 | 41649,40 | 29 | 12,4 |
| 60,01 | 27,32 | 46269,56 | 28,56 | 5,65 |
| 59,84 | 27,25 | 46135,58 | 28,35 | 5,18 |
| 60,10 | 27,37 | 46339,07 | 28,2 | 4,46 |
| 62,37 | 28,40 | 48084,21 | 28,01 | 2,87 |
| 61,25 | 27,89 | 47221,07 | 28,01 | 2,6 |
| 58,23 | 26,51 | 44898,19 | 30 | 8,44 |
| 57,42 | 26,15 | 44274,54 | 30,2 | 9,7 |
| 56,41 | 25,68 | 43491,90 | 24,4 | 12,2 |
| 54,79 | 24,95 | 42246,51 | 22,2 | 13,2 |
| 55,73 | 25,38 | 42970,32 | 22,6 | 12,5 |
| 56,40 | 25,68 | 43482,17 | 22,5 | 11,6 |
| 56,89 | 25,90 | 43865,40 | 29,3 | 11,4 |
| 56,86 | 25,89 | 43840,59 | 29 | 11,7 |
| 56,67 | 25,80 | 43690,71 | 28,3 | 11,7 |
| 55,12 | 25,10 | 42498,08 | 17,5 | 13,6 |
| 54,98 | 25,03 | 42386,78 | 15,4 | 13,8 |

## 7.7 Measurement Matrix sheet

| PIV | Fan | | Vol.flow | | Nozzle | | Re | Vortex | Plane |
|---|---|---|---|---|---|---|---|---|---|
| Index | axial | tang. | axial | tang. | $\Sigma$ Vol.flow | Mean Velo. | | $S_{local}$ | -wise |
| | mVDC | mVDC | kg/h | kg/h | kg/h | m/s | | | |
| offset | -1 | -43 | | | | | | | stream |
| 105 | 70 | 69 | 29,01 | 28,71 | 57,72 | 26,28 | 44501,24 | 0,6 | |
| 106 | 43 | 95 | 23,34 | 31,57 | 54,91 | 25,00 | 42332,91 | 0,8 | |
| 107 | 26 | 150 | 18,69 | 36,77 | 55,46 | 25,25 | 42759,94 | 1,2 | |
| 108 | 26 | 152 | 18,69 | 36,94 | 55,63 | 25,33 | 42893,10 | 1,2 | |
| | | | | | | | | | |
| offset | 0 | -47 | | | | | | | cross |
| 124 | 18 | 186 | 15,55 | 40,05 | 55,60 | 25,32 | 42868,17 | 1.2 | x=2d |
| 125 | 18 | 186 | 15,55 | 40,05 | 55,60 | 25,32 | 42868,17 | 1.2 | x=3d |
| 126 | 18 | 186 | 15,55 | 40,05 | 55,60 | 25,32 | 42868,17 | 1.2 | x=4d |
| 127 | 18 | 186 | 15,55 | 40,05 | 55,60 | 25,32 | 42868,17 | 1.2 | x=5d |
| 128 | 18 | 186 | 15,55 | 40,05 | 55,60 | 25,32 | 42868,17 | 1.2 | x=6d |
| 129 | 18 | 186 | 15,55 | 40,05 | 55,60 | 25,32 | 42868,17 | 1.2 | x=7d |
| 130 | 18 | 186 | 15,55 | 40,05 | 55,60 | 25,32 | 42868,17 | 1.2 | x=8d |
| 131 | 18 | 186 | 15,55 | 40,05 | 55,60 | 25,32 | 42868,17 | 1.2 | x=9d |
| 132 | 18 | 186 | 15,55 | 40,05 | 55,60 | 25,32 | 42868,17 | 1.2 | x=10d |
| 133 | 18 | 186 | 15,55 | 40,05 | 55,60 | 25,32 | 42868,17 | 1.2 | x=11d |
| 134 | 18 | 186 | 15,55 | 40,05 | 55,60 | 25,32 | 42868,17 | 1.2 | x=12d |
| 135 | 18 | 186 | 15,55 | 40,05 | 55,60 | 25,32 | 42868,17 | 1.2 | x=13d |
| 136 | 18 | 186 | 15,55 | 40,05 | 55,60 | 25,32 | 42868,17 | 1.2 | x=14d |
| 137 | 18 | 186 | 15,55 | 40,05 | 55,60 | 25,32 | 42868,17 | 1.2 | x=15d |
| 138 | 18 | 186 | 15,55 | 40,05 | 55,60 | 25,32 | 42868,17 | 1.2 | x=16d |
| 139 | 18 | 186 | 15,55 | 40,05 | 55,60 | 25,32 | 42868,17 | 1.2 | x=18d |
| offset | -1,3 | -47,5 | | | | | | | |
| 156 | 0 | 320 | 4,71 | 49,27 | 53,98 | 24,58 | 41619,46 | 0.8 | x=1d |
| 157 | 0 | 320 | 4,71 | 49,27 | 53,98 | 24,58 | 41619,46 | 0.8 | x=2d |
| 158 | 0 | 320 | 4,71 | 49,27 | 53,98 | 24,58 | 41619,46 | 0.8 | x=3d |
| 159 | 0 | 320 | 4,71 | 49,27 | 53,98 | 24,58 | 41619,46 | 0.8 | x=4d |
| 160 | 0 | 320 | 4,71 | 49,27 | 53,98 | 24,58 | 41619,46 | 0.8 | x=5d |
| 161 | 0 | 320 | 4,71 | 49,27 | 53,98 | 24,58 | 41619,46 | 0.8 | x=6d |
| 162 | 0 | 320 | 4,71 | 49,27 | 53,98 | 24,58 | 41619,46 | 0.8 | x=7d |
| 163 | 0 | 320 | 4,71 | 49,27 | 53,98 | 24,58 | 41619,46 | 0.8 | x=8d |
| 164 | 0 | 320 | 4,71 | 49,27 | 53,98 | 24,58 | 41619,46 | 0.8 | x=9d |
| 165 | 0 | 320 | 4,71 | 49,27 | 53,98 | 24,58 | 41619,46 | 0.8 | x=10d |
| 166 | 0 | 320 | 4,71 | 49,27 | 53,98 | 24,58 | 41619,46 | 0.8 | x=11d |
| 167 | 0 | 320 | 4,71 | 49,27 | 53,98 | 24,58 | 41619,46 | 0.8 | x=12d |
| 168 | 0 | 320 | 4,71 | 49,27 | 53,98 | 24,58 | 41619,46 | 0.8 | x=13d |
| 169 | 0 | 320 | 4,71 | 49,27 | 53,98 | 24,58 | 41619,46 | 0.8 | x=14d |
| 170 | 0 | 320 | 4,71 | 49,27 | 53,98 | 24,58 | 41619,46 | 0.8 | x=15d |

| | | | | | | | | | |
|---|---|---|---|---|---|---|---|---|---|
| 171 | 0 | 320 | 4,71 | 49,27 | 53,98 | 24,58 | 41619,46 | 0.8 | x=16d |
| 172 | 0 | 320 | 4,71 | 49,27 | 53,98 | 24,58 | 41619,46 | 0.8 | x=18d |
| offset | 0 | -48 | | | | | | | |
| 175 | 52 | 95 | 25,18 | 32,08 | 57,26 | 26,07 | 44149,39 | 0.6 | x=1d |
| 176 | 52 | 95 | 25,18 | 32,08 | 57,26 | 26,07 | 44149,39 | 0.6 | x=2d |
| 177 | 52 | 95 | 25,18 | 32,08 | 57,26 | 26,07 | 44149,39 | 0.6 | x=3d |
| 178 | 52 | 95 | 25,18 | 32,08 | 57,26 | 26,07 | 44149,39 | 0.6 | x=4d |
| 179 | 52 | 95 | 25,18 | 32,08 | 57,26 | 26,07 | 44149,39 | 0.6 | x=5d |
| 180 | 52 | 95 | 25,18 | 32,08 | 57,26 | 26,07 | 44149,39 | 0.6 | x=6d |
| 181 | 52 | 95 | 25,18 | 32,08 | 57,26 | 26,07 | 44149,39 | 0.6 | x=7d |
| 182 | 52 | 95 | 25,18 | 32,08 | 57,26 | 26,07 | 44149,39 | 0.6 | x=8d |
| 183 | 52 | 95 | 25,18 | 32,08 | 57,26 | 26,07 | 44149,39 | 0.6 | x=9d |
| 184 | 52 | 95 | 25,18 | 32,08 | 57,26 | 26,07 | 44149,39 | 0.6 | x=10d |
| 185 | 52 | 95 | 25,18 | 32,08 | 57,26 | 26,07 | 44149,39 | 0.6 | x=11d |
| 186 | 52 | 95 | 25,18 | 32,08 | 57,26 | 26,07 | 44149,39 | 0.6 | x=12d |
| 187 | 52 | 92 | 25,18 | 31,78 | 56,95 | 25,93 | 43912,14 | 0.6 | x=13d |
| 188 | 52 | 92 | 25,18 | 31,78 | 56,95 | 25,93 | 43912,14 | 0.6 | x=14d |
| 189 | 52 | 95 | 25,18 | 32,08 | 57,26 | 26,07 | 44149,39 | 0.6 | x=15d |
| 190 | 52 | 95 | 25,18 | 32,08 | 57,26 | 26,07 | 44149,39 | 0.6 | x=16d |
| 191 | 52 | 95 | 25,18 | 32,08 | 57,26 | 26,07 | 44149,39 | 0.6 | x=18d |